AD-A184 412 THE USE OF HOT-FILM TECHNIQUE FOR BOUNDARY LAYER STUDIES ON A 21% THICK AIRFOIL(U) NATIONAL AERONAUTICAL ESTABLISHMENT OTTAWA (ONTARIO) M KHALID MAY 87 1/1

UNCLASSIFIED NAE-AN-45 NRC-27892 F/G 20/4 NL

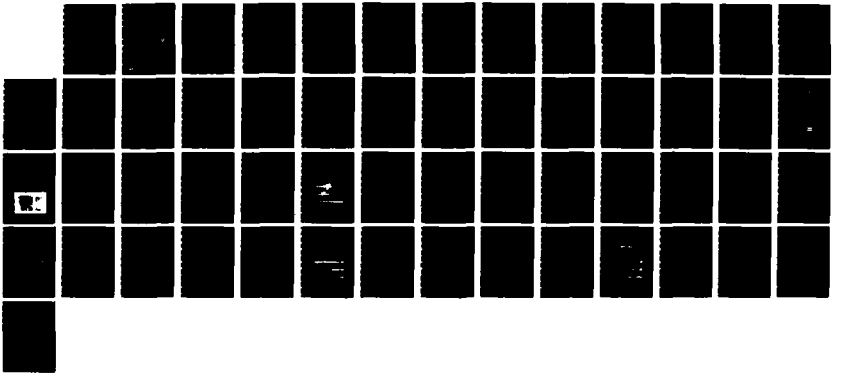

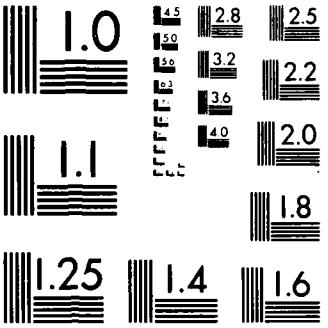

MICROCOPY RESOLUTION TEST CHART
NATIONAL BUREAU OF STANDARDS-1963-A

UNLIMITED
UNCLASSIFIED

Canada

(6)

THE USE OF HOT-FILM TECHNIQUE FOR BOUNDARY LAYER STUDIES ON A 21% THICK AIRFOIL

by

M. Khalid
National Aeronautical Establishment

AERONAUTICAL NOTE
NAE-AN-45
NRC NO. 27892

OTTAWA
MAY 1987

National Research Council Canada
Conseil national de recherches Canada

NATIONAL AERONAUTICAL ESTABLISHMENT

SCIENTIFIC AND TECHNICAL PUBLICATIONS

AERONAUTICAL REPORTS:

Aeronautical Reports (LR): Scientific and technical information pertaining to aeronautics considered important, complete, and a lasting contribution to existing knowledge.

Mechanical Engineering Reports (MS): Scientific and technical information pertaining to investigations outside aeronautics considered important, complete, and a lasting contribution to existing knowledge.

AERONAUTICAL NOTES (AN): Information less broad in scope but nevertheless of importance as a contribution to existing knowledge.

LABORATORY TECHNICAL REPORTS (LTR): Information receiving limited distribution because of preliminary data, security classification, proprietary, or other reasons.

Details on the availability of these publications may be obtained from:

Publications Section,
National Research Council Canada,
National Aeronautical Establishment,
Bldg. M-16, Room 204,
Montreal Road,
Ottawa, Ontario
K1A 0R6

ÉTABLISSEMENT AÉRONAUTIQUE NATIONAL

PUBLICATIONS SCIENTIFIQUES ET TECHNIQUES

RAPPORTS D'AÉRONAUTIQUE

Rapports d'aéronautique (LR): Informations scientifiques et techniques touchant l'aéronautique jugées importantes, complètes et durables en termes de contribution aux connaissances actuelles.

Rapports de génie mécanique (MS): Informations scientifiques et techniques sur la recherche externe à l'aéronautique jugées importantes, complètes et durables en termes de contribution aux connaissances actuelles.

CAHIERS D'AÉRONAUTIQUE (AN): Informations de moindre portée mais importantes en termes d'accroissement des connaissances.

RAPPORTS TECHNIQUES DE LABORATOIRE (LTR): Informations peu disséminées pour des raisons d'usage secret, de droit de propriété ou autres ou parce qu'elles constituent des données préliminaires.

Les publications ci-dessus peuvent être obtenues à l'adresse suivante:

Section des publications
Conseil national de recherches Canada
Établissement aéronautique national
Im. M-16, pièce 204
Chemin de Montréal
Ottawa (Ontario)
K1A 0R6

UNLIMITED
UNCLASSIFIED

THE USE OF HOT-FILM TECHNIQUE FOR BOUNDARY LAYER STUDIES ON A 21% THICK AIRFOIL

UTILISATION DE LA TECHNIQUE DU FILM CHAUD POUR DES ÉTUDES DE COUCHE LIMITE AUTOUR D'UN PROFIL D'AILE D'UNE ÉPAISSEUR RELATIVE DE 21%

by/par

M. Khalid

National Aeronautical Establishment

OTTAWA
MAY 1987

AERONAUTICAL NOTE
NAE-AN-45
NRC NO. 27892

L.H. Ohman, Head/Chef
High Speed Aerodynamics Laboratory/
Laboratoire d'aérodynamique à hautes vitesses

G.F. Marsters
Director/Directeur

SUMMARY

A heat transfer method of studying boundary layer flows over airfoils at transsonic test conditions has been investigated. The method employs very thin DISA hot-film gauges housing Constant Temperature Anemometer probes. Provided that the thickness dimension of the films remains less than the critical disturbances height for inducing transition of the laminar boundary layer, the heat transfer response from the films, positioned carefully on the model surface, can be studied to determine the boundary layer characteristics. Results from an application study on a 21% thick laminar flow airfoil model are presented and discussed.

RÉSUMÉ

La recherche porte sur une méthode de transfert de chaleur utilisée pour l'étude des écoulements dans la couche limite autour de profils d'aile placés dans des conditions d'essais transsoniques. Dans cette méthode, on emploie des manomètres à film chaud DISA très fins logeant des anémomètres à fil chaud à température constante. Si l'épaisseur des films reste inférieure à la hauteur critique des perturbations induisant une transition de la couche limite laminaire, on peut étudier la réponse thermique des films, soigneusement placés à la surface de la maquette, pour déterminer les caractéristiques de la couche limite. Les résultats d'une étude avec une maquette de profil d'aile à écoulement laminaire d'une épaisseur relative de 21% sont présentés et commentés.

CONTENTS

ILLUSTRATIONS

CONTENTS (Cont'd)

CONTENTS (Cont'd)

1. INTRODUCTION

The NAE 21% thick supercritical airfoil 68-060-21:1 has shown some remarkable low drag characteristics as demonstrated by measurements on a 10 inch chord model in the NAE High Reynolds number 2-D facility, Refs. [1,2]. It is reasonable to assume that the low drag features are a result of significant extents of laminar boundary layer over the airfoil. The purpose of the present investigation was primarily to verify the extent of laminar flow by measurements with hot-film gauges, and to demonstrate in general the applicability of some relatively new type of hot-film gauges.

The hot-film method of studying boundary layer characteristics has been used successfully in the past. Owen et al [3] used this technique to measure transition on a cone at hypersonic Mach numbers. Peake et al [4] and Ohman [5] used "McCroskey" hot-film gauges in their supersonic and transonic boundary layer studies at the High Speed Aerodynamics Laboratory of NAE. More recently, in another similar study Fancher (McDonnell-Douglas) [6] investigated the hot-film technique to detect transition using NAE's 2-D High Reynolds Number Test Facility. In this study the gauge elements were vacuum deposited on a very thin dielectric substrate, providing a virtually non-intrusive installation to boundary layers.

The new polyimide, glue-on DISA hot-film probes used in the present experiment have been manufactured sufficiently thin to be almost non-intrusive and sensitive enough to be able to measure heat-transfer rates at transonic Mach numbers. The measure of heat transfer rate as detected by the DISA hot-film strips, mounted at strategic

locations on the model surface provided continuous information on the boundary layer conditions.

The data recorded from the hot-film strips was studied in light of the chordwise pressure distribution measurements and in one instance with some flow visualization snap shots.

This report discusses some interesting features of the data collected. For a number of runs, chordwise pressure measurements from the model surface as well as the normalized R.M.S. output of the heat transfer rate are provided in a graphical format. To show certain trends in data the AC signals, and in some cases the R.M.S. levels of the signals and their spectra are also shown.

2. DESCRIPTION OF THE EXPERIMENT

2.1 Facility

The investigation was carried out in the NAE's 15" × 60" High Reynolds Number 2-D Facility, [7]. For a description of the equipment, instrumentation and data reduction related to balance and pressure measurements the reader is referred to Ref. [8]. Only the DISA hot-film related aspects of instrumentation and data reduction will be dealt with here.

2.2 Model

A 21% thickness to chord ratio supercritical model NAE 68-060-21:1 having a chord length of 9.9937 inches (shown in Figure 1) was suitably instrumented for this investigation. Having

experimented twice with this model for other aerodynamic purposes [8,9] and developed a familiarity with its performance were part of the reason for choosing this model for the present study. It was manufactured in the NAE's HSAL machine shop. The model is made of aluminum and has been given a surface treatment (anodized) which gives the model a shiny black smooth surface. The surface smoothness was measured to be within an RMS value of 12×10^{-6} to 17.6×10^{-6} inches. The model was equipped to provide chordwise pressure distribution measurements, see Ref. [8].

For the ease of accessing wires from the hot-film probes planted on the model surface, the model was installed inverted in the tunnel.

2.3 The DISA Hot-film Probes

The DISA hot-films were 0.63 inches in length, 0.315 inches wide and 1.97×10^{-3} inches thick. They were made from a polyimide material and had 1.97×10^{-4} inches thick quartz coating. The actual constant temperature anemometer (CTA) nickel probe housed within the film had dimensions of 3.54×10^{-2} inches $\times$ 3.937×10^{-3} inches $\times$ 1.97×10^{-4} inches. The films were glued on to the model upper surface using Eastman 910 adhesive at six predetermined locations. The thickness of the hot-films was close to the permissible thickness [10] which may force transition. For example, at a Reynolds number of R/ft = 8×10^{6}, a disturbance thickness of 2.086×10^{-3} inches placed at a distance of 1.5 inches from the leading edge will force transition.

The positioning of the hot-film probes was thus schemed carefully. The arrangement shown in Figure (2) was designed such that no one probe would be affected by any disturbances emanating from an upstream probe or even the side wall boundary layer. The

wires from each probe were pulled back along the top surface towards the trailing edge. They were then worked round the trailing edge and turned at right angles towards the south wall (model inverted) end of the model. The wires were finally worked out of a clearance next to the pressure connector and taken to the DISA anemometer, a linearizer and RMS measuring units. The DISA hot-film and accessory units had been calibrated according to the procedure described in Ref. [11,12]. The DISA hot-film instrumentation on the model is shown in Figure (3). See bottom of Figure 3 for a brief description of the probes.

The block diagram in Figure (3) shows how the signal from the hot film-constant temperature anemometer was processed. The DC component of the signal was obtained through a low pass filter to provide a mean output. The root mean square (RMS) value of the AC signal was measured using an RMS meter after it has passed through a high pass filter. The amplified AC signal from the high pass filter as well as the wide band signal from the CTA were recorded directly on an FM Tape Recorder and processed using a FFT analyser.

The tare value measured at wind off conditions for the DC signal was the mean value (VDT) whilst the tare value for the RMS signal was the mean value squared (VMT). For every wind-on α-step the following information was computed for each hot-film probe:

VDN - DC mean value per α-scan

VMR - (mean RMS value per α-scan)^2

DVN = VDN - VDT

RMN = $\sqrt{(VMR - VMT)}$

R_N = RMN/DVN (normalized RMS)

The measure of R_N from the six flush mounted probes placed at different axial stations provided an indication of the state of the boundary layer along the model surface.

In physical terms the DC value DVN refers to a measure of steady thermodynamic properties in the flow and RMN refers to the fluctuating component of the same properties. In laminar flow the RMN value is very small and the resulting R_N value therefore is very low. In the transition regions the fluctuating signal RMN is very large compared to the steady state value DVN giving rise to a large peak value of the R_N signal. In the turbulent region, both RMN and DVN are large, making their ratio R_N relatively smaller.

3. TEST PROGRAM

This test program comprised of eleven runs in which the flow conditions were varied according to the following ranges:

Mach Number Range	0.6	$\leq$	M	≤ 0.7
Reynolds Number Range	4.17×10^6	$\leq$	R_C	$\leq 9.2 \times 10^6$
Incidence Range	-3.5 deg	$\leq$	α_{COR}	≤ 4.28 deg
Total Pressure	19.48 psia	$\leq$	P_o	≤ 45.63 psia

α_{COR} - incidence corrected for wall interference

R_C - Reynolds number based on model chord

4. DISCUSSION OF RESULTS

Figures (4a), (4b) and (4c) show the normalized RMS values of the heat-transfer rates output R_N = RMN/DVN as measured by the six flush mounted DISA probes during three consecutive pressure scans at constant flow conditions. Each scan was of 2.5 seconds duration which

also was the sample time of the hot-film signals. The test conditions were M = 0.68, $R_C = 6.65 \times 10^6$ and $\alpha_{COR} = -0.27$.

The hot-film data were complemented with a separate flow visualization run, the result of which is shown in Figure (4d). The three sets of hot-film data show good consistency.

The output from the six probes (Figures (4a,b,c)) with the flow conditions being at M = 0.68 and $R_C = 6.65 \times 10^6$ and $\alpha_{COR} = -0.27°$ represents a classic picture of a boundary layer development. The first three probes measure negligible R_N output signifying laminar flow. This is followed by a sharp rise in R_N output reaching a maximum around the fourth probe, depicting transition peak in between 45 to 50% of the chord length. The P_4 values show some variations which are indicative of that transition is not a steady phenomenon. The steady decline in the normalized heat transfer rate output R_N as seen by the fifth (P_5) and sixth (P_6) probe represents the turbulent nature of the flow. This type of boundary layer response as seen by the flush mounted hot-films has also been established for supersonic and hypersonic flow see Refs. [3] and [4].

Figure 5 shows the spectra obtained with a digital signal analyser. The FM Racal tape recorder which stored the six signal was run appropriately to permit a frequency response of up to 12.8 kHz. For the entire frequency range 50-12.8 kHz, the first three probes detect a low energy level in the range, $-100.0 < \tilde{E} < -75.0$ (where $\tilde{E}$ is defined as 20 log (RMS volts)/(Ref volt = 1.0)). This appears to suggest that the first three probes must be situated in the laminar region of the boundary layer. The fact that probe 3, $\tilde{E}$ level is lower than the probe 1 and 2 is presumably due to some leading edge acceleration of the flow at the first two probes.

In the frequency range of about 150 ~ 1500 Hz, probes 4 and 5 occupy the highest energy levels. This is presumably due to their proximity with the transition region. At the highest frequency value close to 12.8 kHz, the $\tilde{E}$ level of the last probe P_6 is as high as P_5. The theoretical spectra lines for turbulent flow having slopes of $\eta = -5/3$ and -7 are also shown. It is evident that at lower frequencies 300 ~ 5000 Hz, it is probe 5 which best matches the higher slope ($\eta = -5/3$) line. At the higher frequency range 5000 ~ 10,000 Hz both probes 5 and 6 agree with the $\eta = -7$ slope spectrum line. Thus both probes 5 and 6 are showing strong turbulent flow spectra characteristics.

The pressure trace shown in Figure (6) also shows favourable conditions for laminar flow up to 50% of the chord length. The adverse pressure gradient beyond 55-60% of the chord length would promote turbulent flow on the aft portion of the model upper surface. Whilst it is not possible to establish the onset of transition from pressure traces, it is clear that the inferred laminar and turbulent regions are in harmony with the hot-film findings.

The flow visualization picture shown in Figure (4d) is not so easy to interpret as individual specks of dust on the model surface appear to trip local transition. The small dark shades just aft of P_1 and P_2 are tell tale signs of some local transition. However, a careful examination of the picture around a cleaner portion of the model shows that the flow remained laminar in region 1 which is about 45% of the model chord length. The transition wedges appear in a region 45 to 50% of the chord length. The flow is turbulent past this point in

region 3. Thus the flow visualization pattern is satisfactorily consistent with the hot-film results.

The dark shade close to the leading edge can be attributed to some local phenomenon probably caused by uneven or excessive oil spray application and other 3-D effects.

It is interesting to note that the hot-film data for all three scans have predicted very similar flow patterns on the airfoil surface. The slight difference in absolute output as measured by the last three probes can be attributed primarily to the increasingly unsteady nature of transition. This ability of the probes to respond to the instantaneous local boundary layer conditions will be investigated in some of the forthcoming data.

Figure (7a) shows the normalized R_N hot-film data scanned at twelve angles of attack settings in the range $-3.5 \leq \alpha_{COR} \leq 2.81$ with the other flow conditions being $M = 0.66$ and $R_C = 4.17 \times 10^6$. Figures (7b) and (7c), respectively show the AC signals, and a selection of R.M.S. data from the same run.

Whilst the R_N data Figure (7a) does not show a conclusive transition peak at $\alpha = -3.5$, a glance at the AC signals trends Figure (7b) and R.M.S. data Figure (7c) clearly show that transition must have occurred between P_3 and P_4 in region $0.45 \leq x/c \leq 0.5$. For the angle of attack range $-2.26 \leq \alpha_{COR} \leq -0.17$, the normalized R_N hot film data shows a definite transition peak in the above chordwise range. For higher angles of attack $\alpha_{COR} > -0.17$, the regions of laminar flow appear to become longer as the transition peak moves rearwards. This

behaviour is consistent with the 'bucket phenomenon' observed in Ref. [9] and attributed to the ability of NLF airfoils to sustain relatively long laminar runs at certain conditions.

Figure (7b) shows the AC signal from all six probes for the entire run. It is clear that from the middle of step 2 to step 7, which is the angle of attack range $-2.26 < \alpha_{COR} < -0.17$, probe 4 detects a high level of flow activity. This indicates a transition somewhere in the locality $0.45 < x/c < 0.5$. The large positive spikes in signals at probe 4 and 5 between steps 2 and 7 are indicative of the turbulent nature of the flow, where as the negative spikes represent the laminar tendencies. The two tendencies here are probably responsible for the apparent offset in the mean of the signal. Past step 7, ($\alpha_{COR} > -0.17$) it is the probe 6 which appears to be in the highest activity region and that is most likely associated with incipient trailing edge separation. Both probes 4 and 5 indicate turbulent flow after step 7.

The (RMS) Root Mean Square values of the above signals are also provided (Figure 7c) for at least three steps in the above run. In steps 1 and 9, probe 6 stationed at $x/c = 0.9$ registers the most chaotic conditions most likely signifying an incipient trailing edge separation. The remaining five probes signals exist within a narrow band of 0.009 volts. In step 5, probes 4 and 5 followed by the probe 6 detect the largest RMS levels indicating a transition region in the range $0.45 < x/c < 0.5$. The first three probes show a signal level of about 0.0029 volts, and, presumably, see a stable laminar flow.

We thus observe that the results from the normalized R_N probe data, the AC signal and the R.M.S. data are in good agreement, as

expected. For this particular run the conclusion is that the flow is laminar up to an axial station of x/c = 0.45. It experiences transition in the region $0.45 < x/c < 0.5$, followed by turbulent flow.

The pressure distribution traces given in Figure (7d) correspond to the above hot-film data. These traces, whilst failing to identify the exact transition locations do however substantiate the existence of laminar and turbulent region according to the above description.

To complement the above results a theoretical pressure boundary layer calculation was performed by D. Jones of NAE for two of the above cases, Steps 1 and 2 in Fig. 7a, using a modified BGK non conservative code. The original BGK code [13] has been modifed by including Thwaites' laminar boundary layer method [14] with a compressiblity transformation, the transition prediction method of Cebeci et al [15] and the Green's lag entrainment method [16] for the turbulent boundary layer.

The results of these calculations are shown in Figures 7e and 7f, which show the pressure distribution and the boundary layer shape factor H distribution. The experimental pressure distribution for these two steps is also plotted (see Figure 7g) and agrees reasonably well with calculations, especially so for the upper surface. The transition prediction is for about 60% chord in both cases for the upper surface, which agrees possibly well with the Step 1 data but not with the Step 2 data which show transition at about 45%. It has been observed in other cases as well that the transition prediction method is too optimistic.

Figure (8a) provides the normalized hot-film data R_N at $M = 0.66$ and $R_C = 6.67 \times 10^6$.

An early possible transition peak around x/c = 0.3 is indicated for angles of attack α_{COR} = -3.52 and -2.27. For angles of attack $-1.48 < \alpha_{COR} < 0.16$, no transition peak is detected up to x/c = 0.55. The AC signals for this run shown in Figure (8b) also show a relatively active probe 3 (x/c = 0.3) for the first two steps (α_{COR} = -3.52 and -2.27). Very little AC activity is detected by the first five probes past the second step until α_{COR} = 2.78 is reached, when P_4 becomes noisier.

The pressure distribution traces Figure (8c) also show favourable or constant pressure conditions up to x/c = 0.55 on the upper surface for angle of attack values $-3.52 < \alpha_{COR} < 0.16$. For α_{COR} = 0.6 and 1.02 the traces show negative slopes beyond $x/c \approx 0.1$, and, for three highest incidences they indicate the presence of a shock wave at $x/c \approx 0.3$ to 0.4. In the latter cases one would undoubtedly assume that transition would occur no later than in the shock wave region. However, presumably because of the location of the hot-film gauges they don't pick up any strong transition signal. Only P_4 gives a clear indication of transition for the highest incidence.

Figure (9a) provides the hot-film R_N data at M = 0.7 and $R_C = 6.66 \times 10^6$. Up to an angle of attack value of α_{COR} = 0.54 (except for α_{COR} = -3.55) the peak signal is always centred around x/c = 0.45. For $\alpha_{COR} > 0.54$ the peak moves rearwards to x/c = 0.55. The corresponding AC signals shown in Figure (9b) are consistent with the results of Figure (9a). Note that probe 5 suddenly becomes noisier after step 8 ($\alpha_{COR} > 0.54$).

The pressure traces shown in Figure 9c show favourable conditions until $x/c \approx 0.6$ for the above low angle of attack range

$\alpha_{COR} < 0.54$. However, at the ninth scan, $\alpha_{COR} = 0.97$. There is a distinct jump in the pressure value close to the station $x/c \simeq 0.51$. This type of jump in pressure is indicative of the presence of a shock wave. This also happens to be the scan at which the peak of the signals from the hot-films probes (Fig. 9a) moves rearwards for the first time to $x/c \simeq 0.51$. Thus both methods have successfully confirmed the presence of a shock wave close to the axial station $x/c \simeq 0.51$. This identification of a shock wave location through a comparison of pressure traces and the hot-films signals continues up to an angle of attack value of $\alpha_{COR} = 2.29$. At the highest angle of attack $\alpha_{COR} = 4.27$ the pressure trace begins to show a negative slope as early as the station $x/c = 0.2$. The high level of signals registered by the last three probes are probably due to unsteady flow separation effects (buffetting).

Figure 10a shows the hot-film R_N data at the Mach Number of 0.7 and $R_C = 9.17 \times 10^6$. The corresponding AC signals are presented in Figure 10b.

The second probe registers a signal higher than the adjacent two probes, and it becomes more pronounced with increasing α_{COR}. Although the pressure traces for most scans do not show a negative slope until at least $x/c \sim 0.55$, the high level of activity at probe 2 is indicating an early transition. A glance at the drag performance of this airfoil substantiates this observation, see Runs 29760 and 29770 in Ref. [8]. A rather high drag level of $C_{DW} = 0.0146 \sim 0.0155$ for $C_L < 0.5$ at $R_C = 9.17 \times 10^6$ suggests that the airfoil was experiencing an almost fully turbulent flow.

Similar to the last case discussed, a clear jump in pressure is observed close to the station x/c ≈ 0.51 at the ninth scan in Figure 10c. This type of jump as mentioned before is usually associated with the presence of a shock wave. The hot-film data too, show a relatively higher level of signal (when compared to its lower α readings) close to this station at the ninth scan. Again, both measurement techniques indicate the presence of a shock wave for all increasing incidence cases except the last one. At the last scan α_{COR} = 4.28, the shock wave appears to have been smeared out by the unsteady buffet effect in the flow, as the pressure begins to increase continuously beyond x/c = 0.2. The peak of the R_N signals of the probes also moves ahead of x/c = 0.5 value. Again the last three probes register relatively high signals indicating turbulent unsteady nature of the flow.

For the last two runs investigated it is unlikely that the transition would occur any later than the station where the shock wave is located.

5. CONCLUSIONS

1. Regions of laminar, transition and turbulent flow can be identified by studying hot-film data in conjunction with the pressure traces.
2. It was observed that the boundary layer/shock wave interaction leads to a notably high intensity signal from the hot film guage.
3. To obtain a more detailed chordwise information about the state of the boundary layer it may be necessary to increase the number of hot-films mounted on the airfoil surface.

4. At higher Reynolds Number runs, the hot-films themselves may cause the boundary layer to trip. Some work is planned to investigate if the hot-wire element contained in the film can be epoxy mounted in a recess to minimize the disturbance.

5. For the present 21% thick model NAE 68-060-21:1 it was confirmed that the flow remained laminar for as much as 45% of the chord length close to the design conditions of M = 0.68, C_L = 0.41 and $R_C = 6.65 \times 10^6$.

6. REFERENCES

1. Jones, D.J.; Khalid, M.; 'Analysis of experimental data for a 21% thick natural laminar flow airfoil NAE 68-060-21:1,' NRC Report, Aeronautical Note NAE-AN-34.

2. Eggleston, B.; Jones, D.J.; Poole, R.J.D.; and Khalid, M.; 'Thick Supercritical Airfoils with low Drag and NLF capability,' International Conference of Aeronautical Sciences. London Sept. 1986.

3. Owen, F.K., Horstman, C.C., Stainback, P.C. and Wagner, R.D.; 'Comparison of wind tunnel transition and freestream disturbance measurements,' AIAA, March 1975, pp. 266-270.

4. Peake, D.J.; Bowker, A.J., Lockyear, S.J. and Ellis, F.A.; 'Non-obtrusive detection of transition region using an infrared camera,' AGARD Conference proceedings No. 224. Laminar-Turbulent Transition 2-4 May 1977.

5. Ohman, L.H. 'Investigation of the Onera LC100D Supercritical airfoil at high Reynolds number,' NRC Report LTR-HA-5×5/0083.

6. Fancher, M.F.; 'Aspects of cryogenic wind tunnel testing technology at Douglas,' AIAA 12th Aerodynamic Testing Conference. Williamsburg, March 1982.

7. Ohman, L.H.; 'The NAE high Reynolds number 15" × 60" two dimensional test facility,' NAE LTR-HA-4, April 1970.

8. Khalid, M. and Jones, D.J.; 'Further wind tunnel tests on a 21% thick supercritical airfoil NAE 68-060-21:1, in the NAE 2D facility,' LTR-HA-5×5/0160, May 1986.

9. Khalid, M. and Jones, D.J.; 'Experimental investigation of a 21% thick supercritical airfoil NAE 68-060-21:1 in the 15" × 60" facility,' LTR-HA-5×5/0155, March 1985.

10. Braslow, A.L. and Knox, E.E.; 'Simplified method for determination of critical height of distributed roughness particles for boundary layer transition at Mach Numbers from 0 to 5,' NACA TN 4363, September 1958.

11. Geremia, O.J.; 'Experiments on the calibration of flush mounted film sensors,' DISA Information No. 13, May 1972.

12. DISA Instructions Manuals for CTA Bridge Type 56 C 17, 56 C 01 CTA Singal conditioner 56 N 20, Lineariser 56 N 21, Mean Value Unit 56 N 22, Printed in Denmark (DANTEC).

13. Bauer, F., Garabedian, P., Korn, D.; 'Supercritical wings sections III,' Lecture notes in Economics and Mathemtical Systems, No 150, Springer-Verlag 1977.

14. Thwaites, B., 'Approximate calculation of the laminar boundary layer,' Aeronautical Quarterly Vol. 1., pp 245-280, Nov 1949.

15. Cebeci, T., Mosinski, G.J. and Smith, A.M.O.; 'Calculation of viscous drag and turbulent boundary layer separation on 2-dimensional and axisymmetric bodies in incompressible flows.' Douglas Aircraft Co. Report No. MDC-J0973-01, Long Beach, Calif. 1970.

16. Green, J.E., Weeks, D.J., Brooman, T.W.F.; 'Prediction of turbulent boundary layers and wakes in compressible flow by a lag entrainment method,' RAE TR 72231, January 1973.

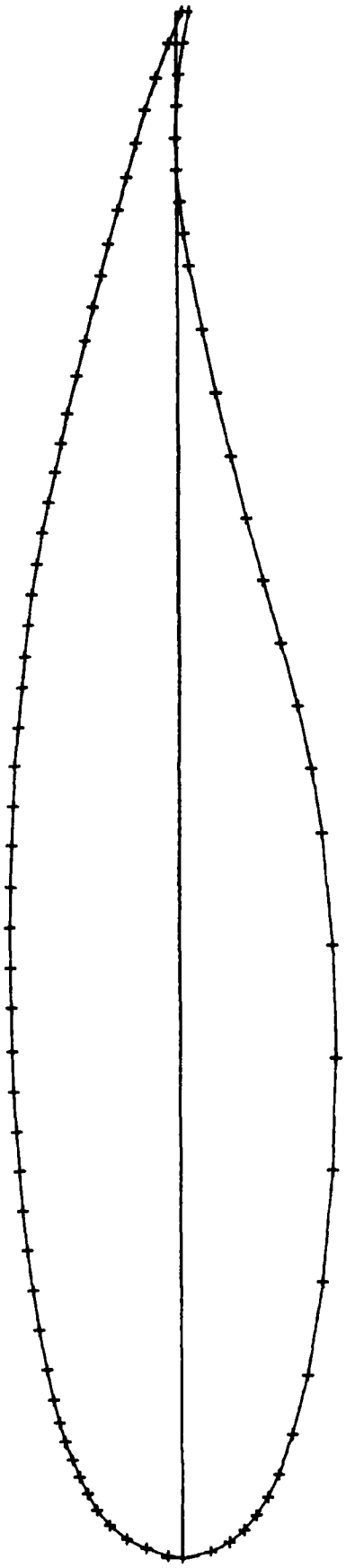

FIG. 1: NAE 68-060-21:1 t/c = 0.21 SUPERCRITICAL MODEL

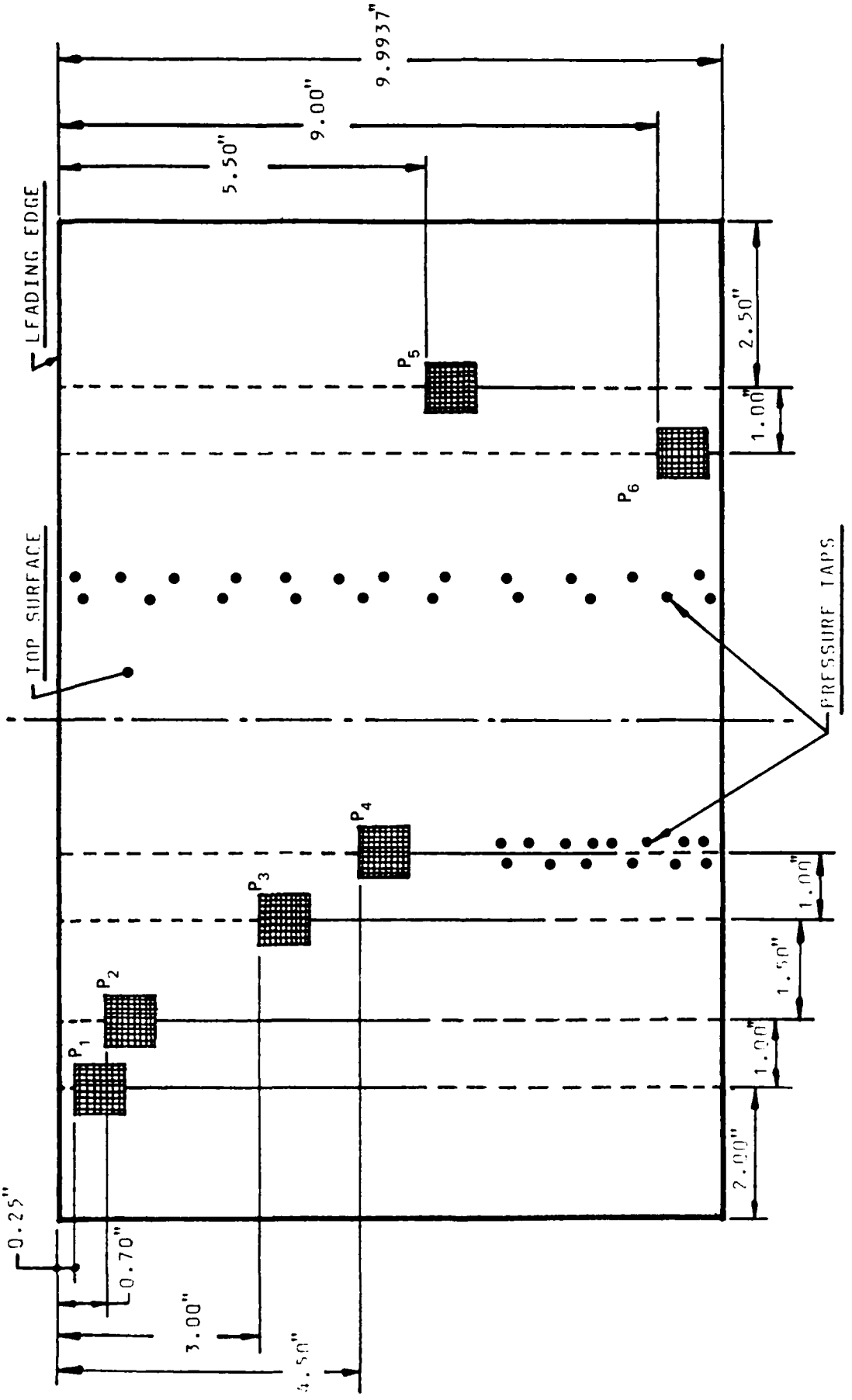

FIG. 2: SCHEME FOR CTA-PROBES INSTALLATION ON MODEL NAE 68-060-21:1

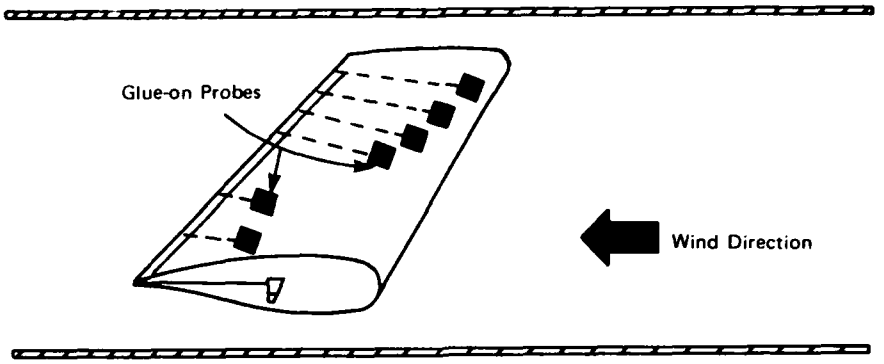

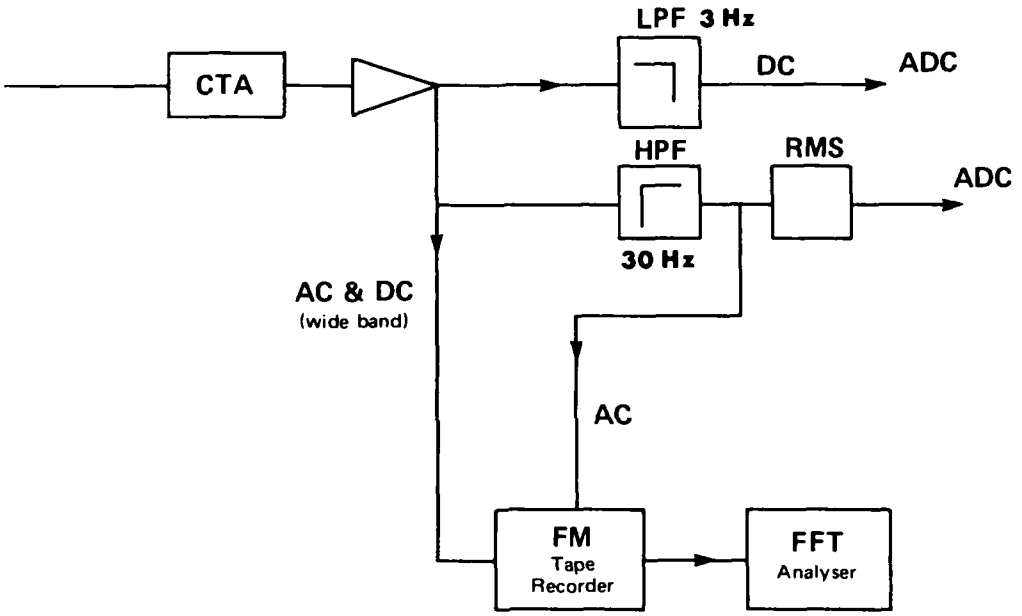

Glue-on Probes

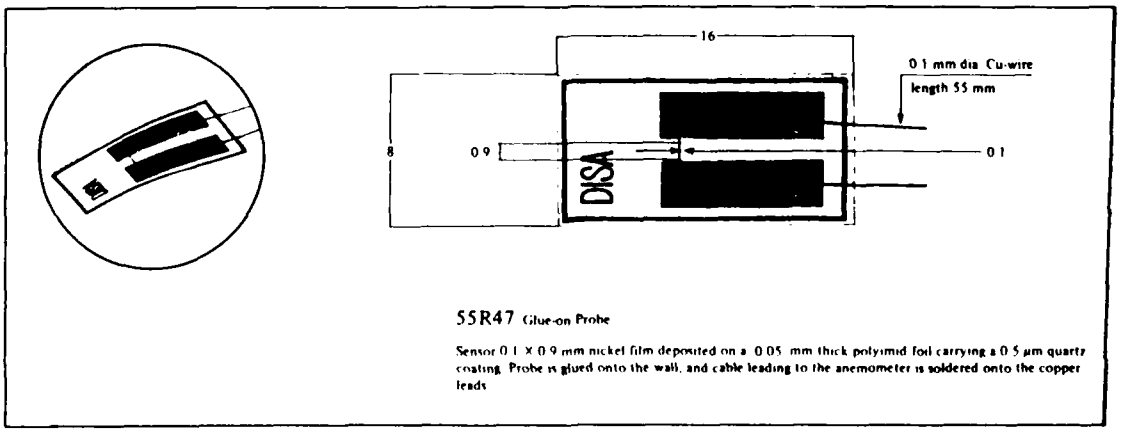

FIG. 3: SKETCH OF THE DISA HOT-FILM INSTRUMENTATION

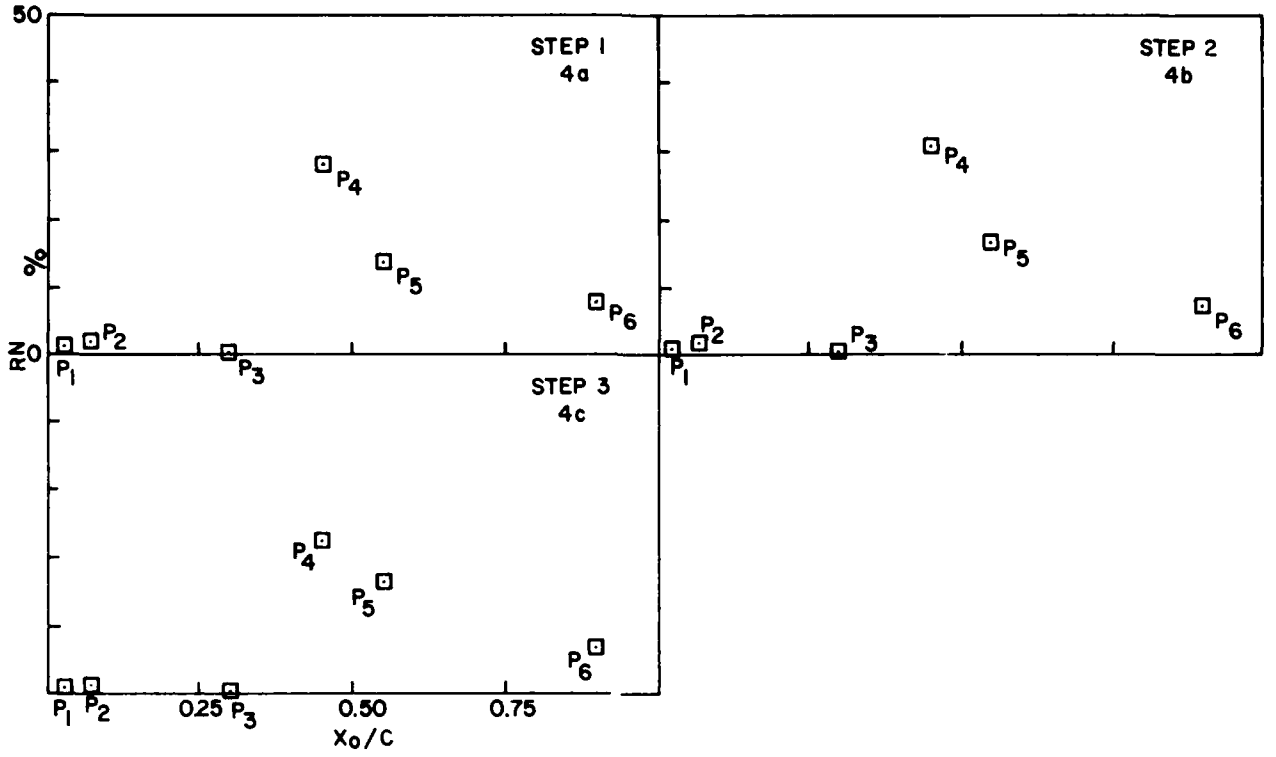

FIG. 4(a), (b), (c): HOT-FILM RECORDS α_{COR} = -0.27, M = 0.68 AND R_C = 6.65 X 10^6

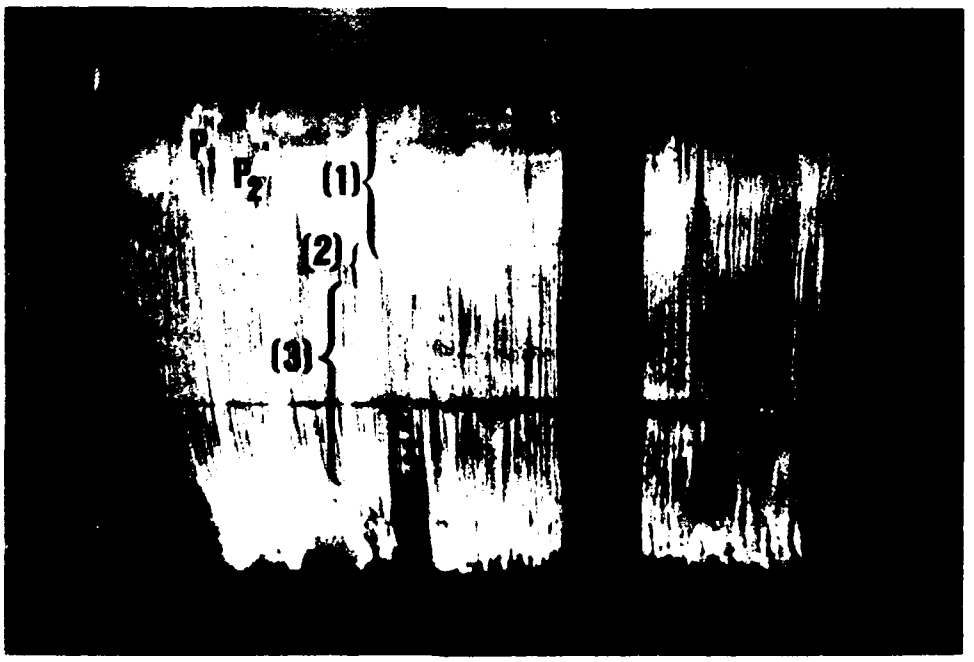

1. LAMINAR 2. TRANSITIONAL 3. TURBULENT

FIG. 4(d): FLOW VISUALIZATION FOR THE ABOVE CASE

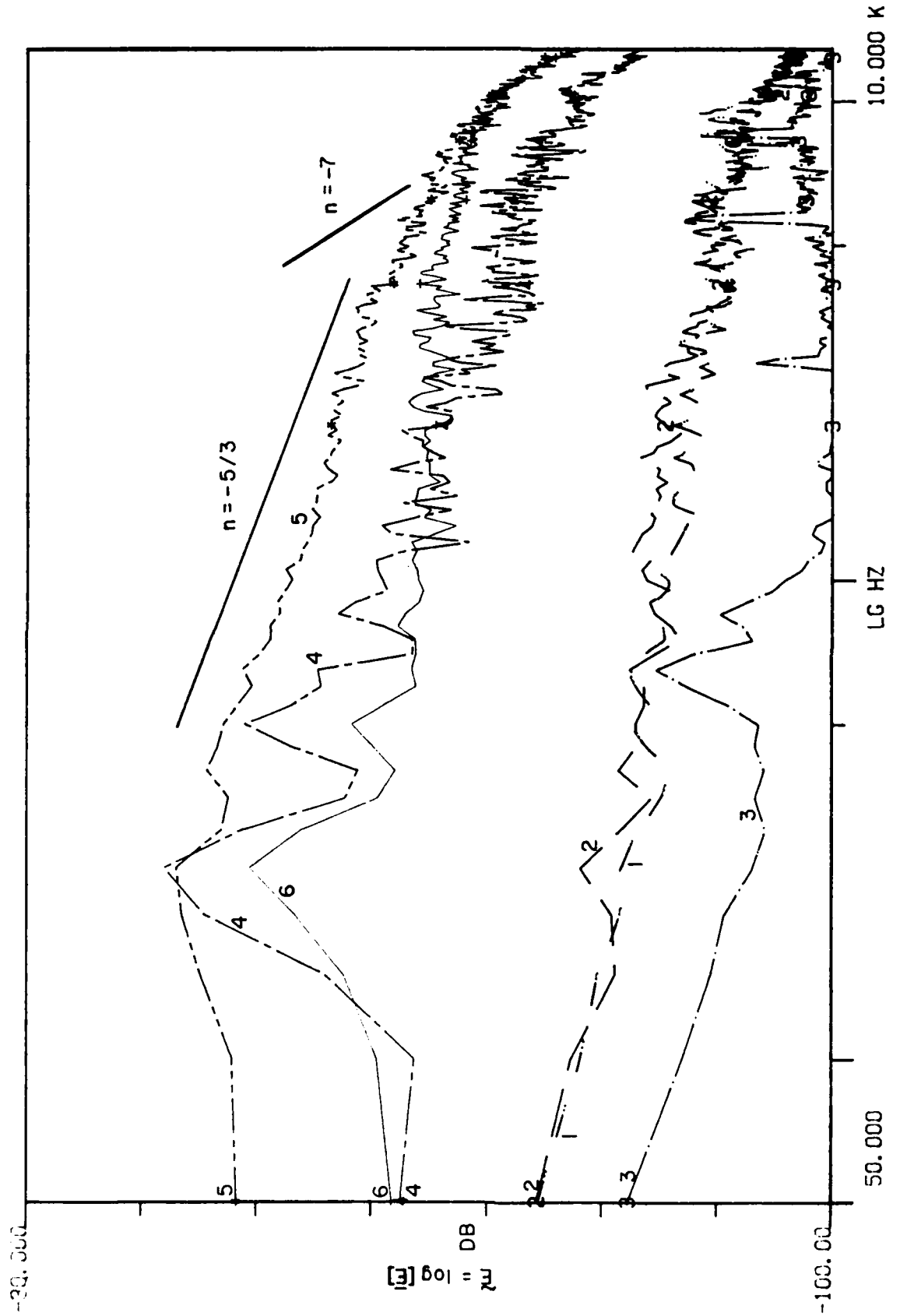

FIG. 5: SPECTRA OF HOT-FILMS; M = 0.68, $R_C = 6.65 \times 10^6$ AND $\alpha_{COR} = -0.27$

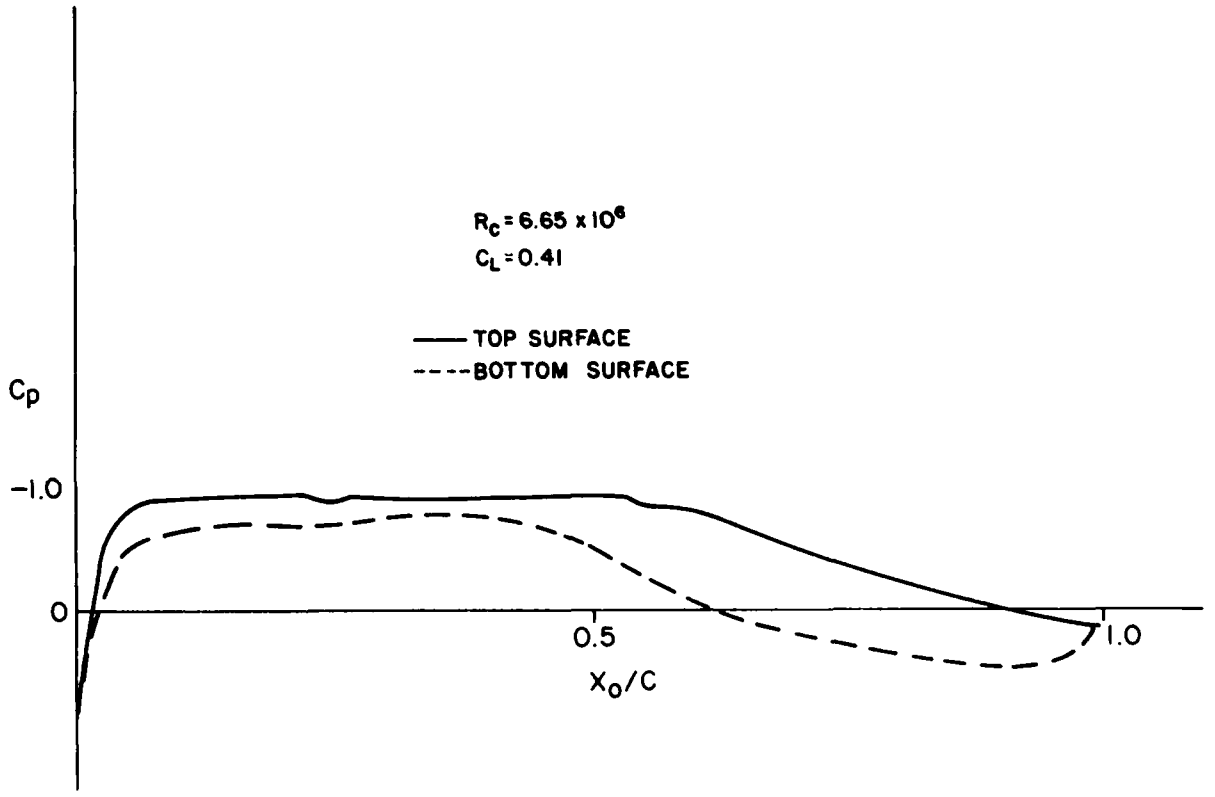

FIG. 6: CHORDWISE MEASURED PRESSURE DISTRIBUTION M = 0.68, α_{COR} = -0.27

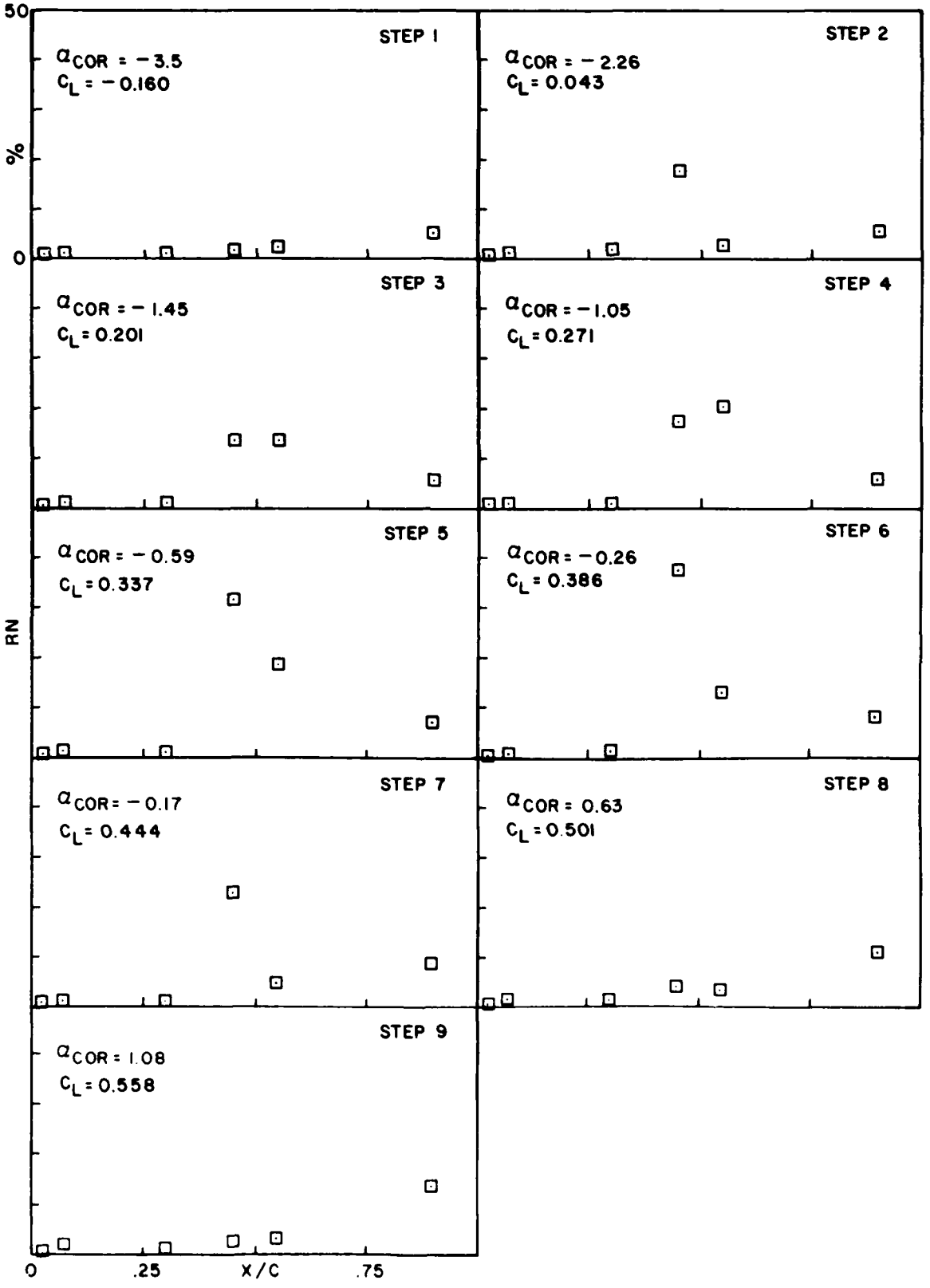

FIG. 7(a): HOT-FILM RECORDS $-3.5 \leq \alpha_{COR} \leq 2.81$, M = 0.66 AND $R_C = 4.17 \times 10^6$

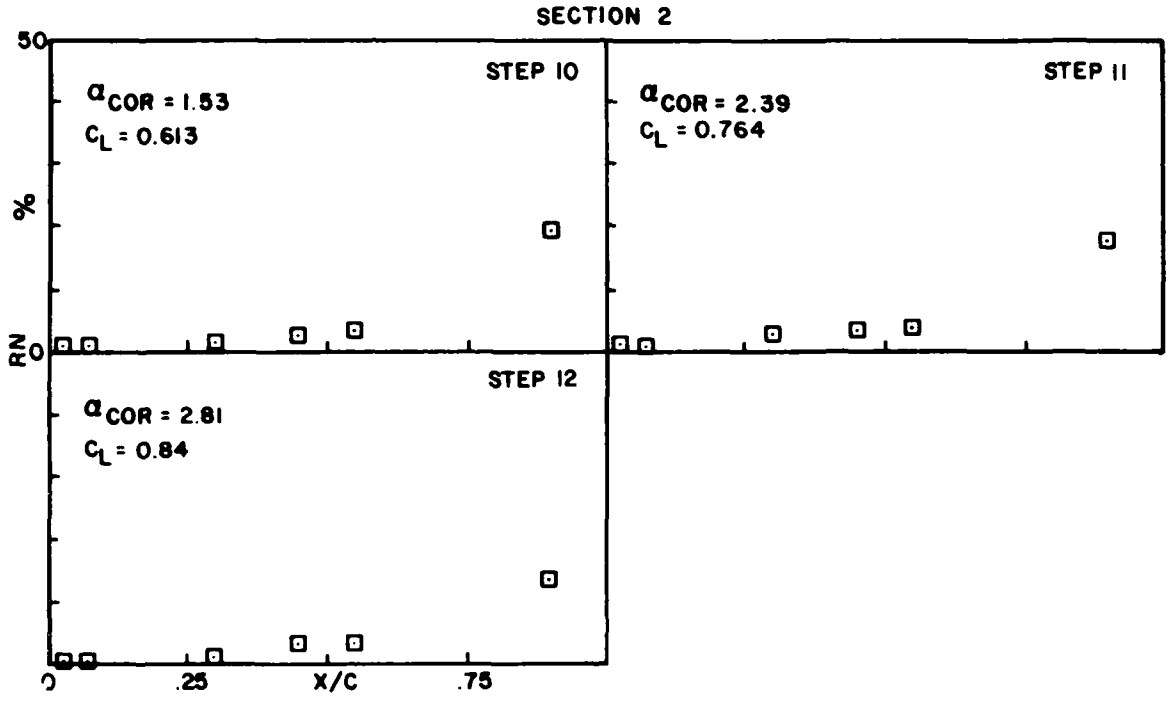

FIG. 7(a) (cont'd): HOT-FILM RECORDS $-3.5 \leqslant \alpha_{COR} \leqslant 2.81$, M = 0.66 AND $R_C = 4.17 \times 10^6$

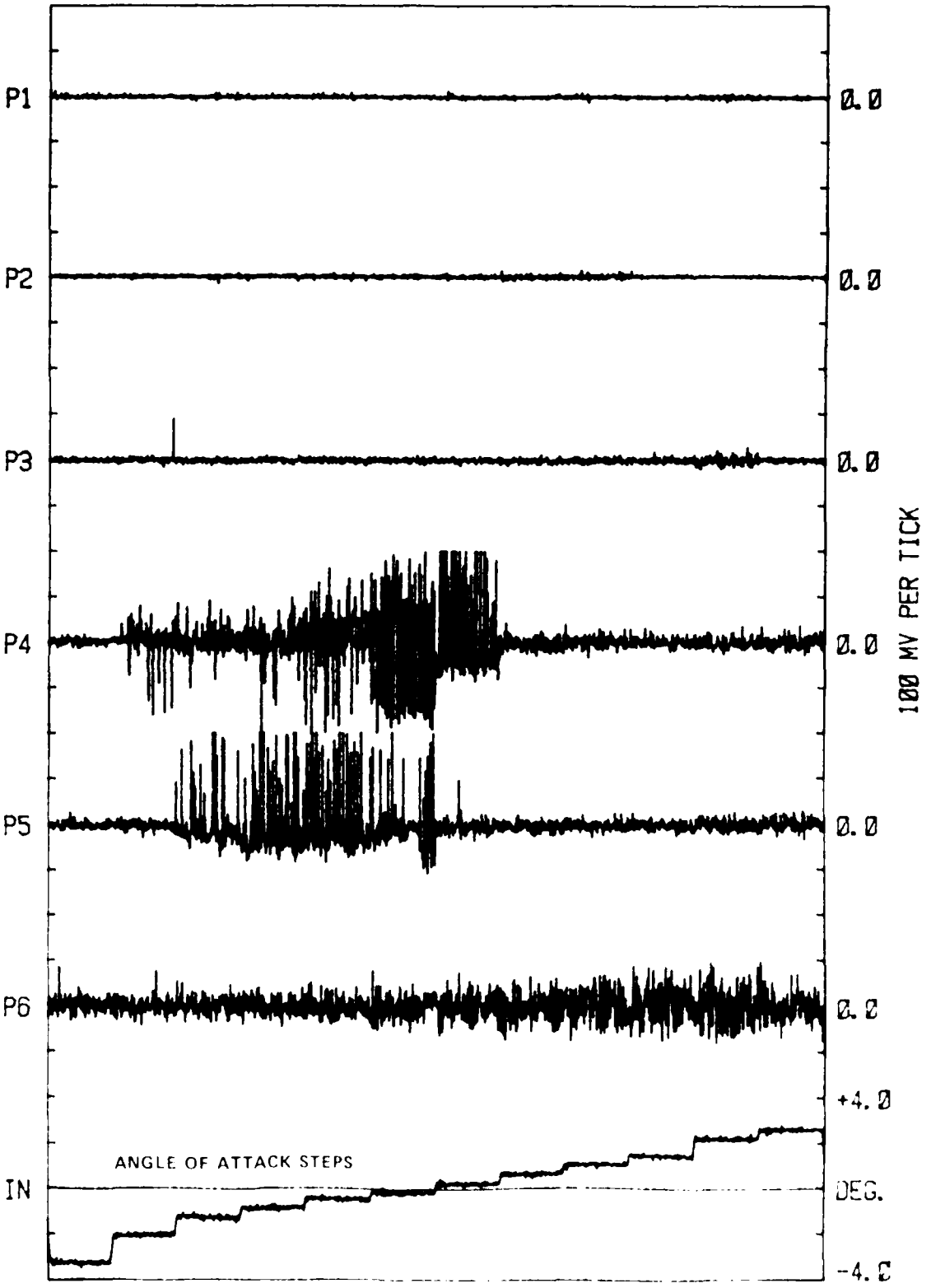

FIG. 7(b): THE AC SIGNAL FROM THE DISA HOT-FILM PROBES

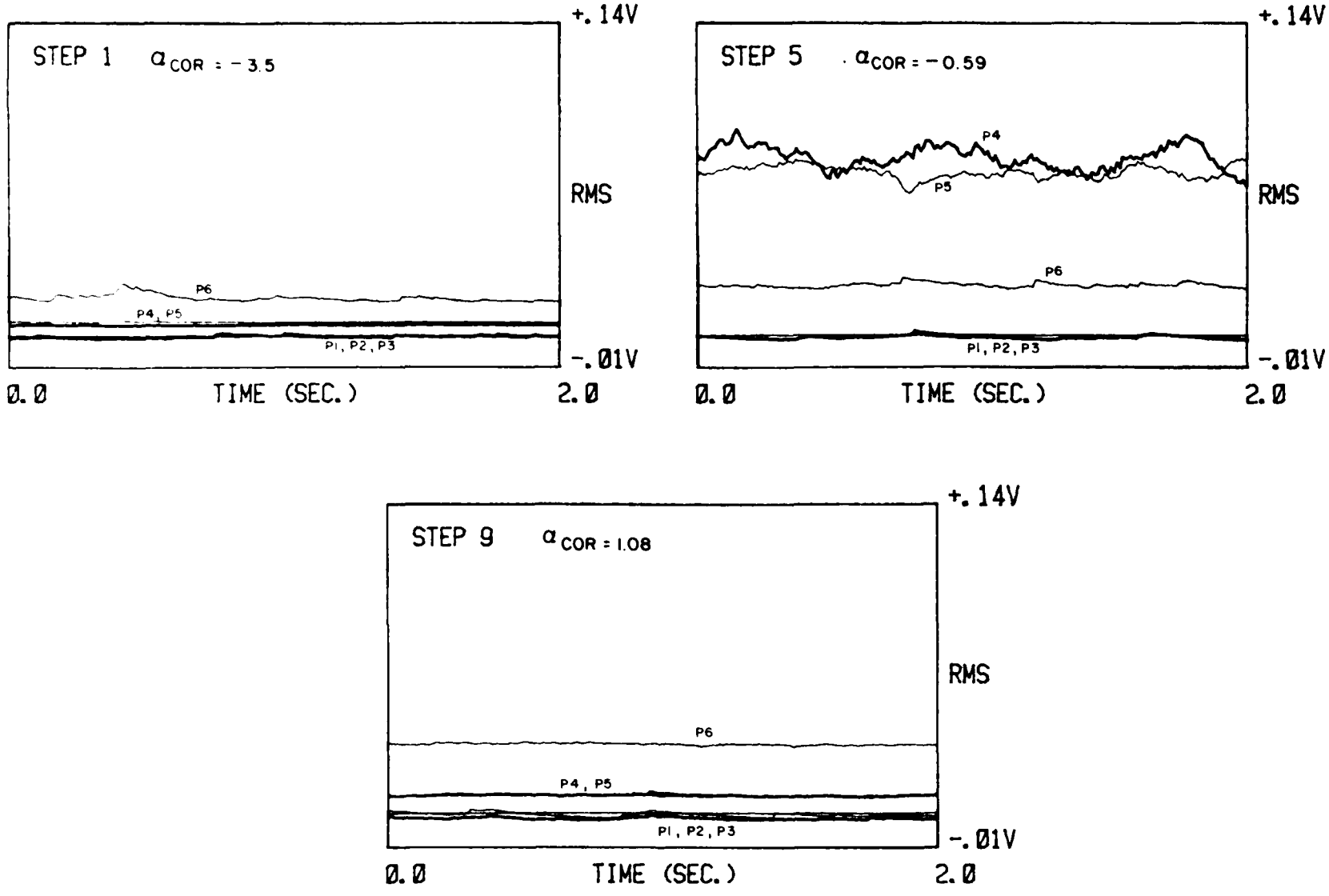

FIG. 7(c): THE RMS SIGNAL FROM THE DISA HOT-FILM PROBES

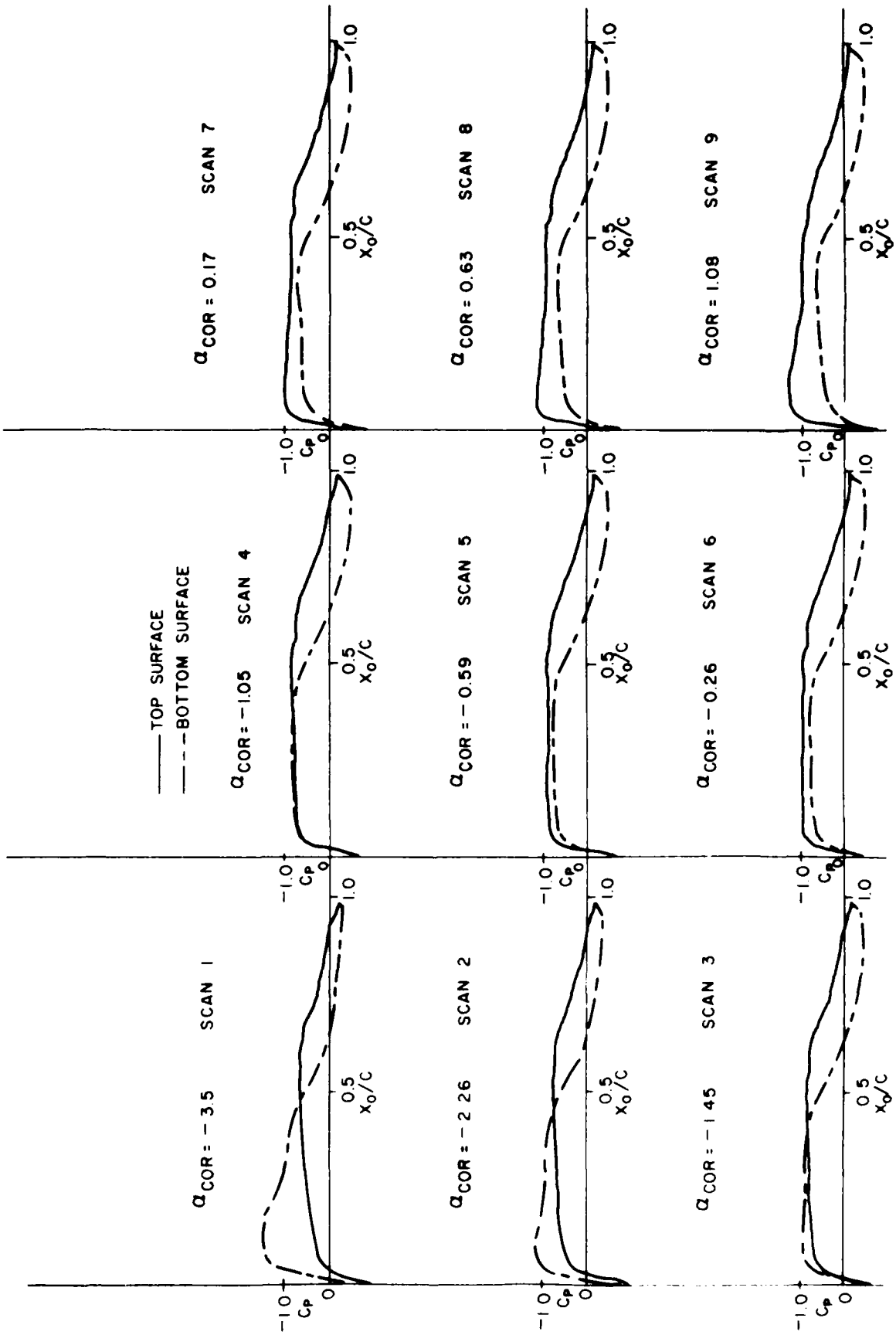

FIG. 7(d): CHORDWISE MEASURED PRESSURE DISTRIBUTION M = 0.66, R_C = 4.17 X 10^6

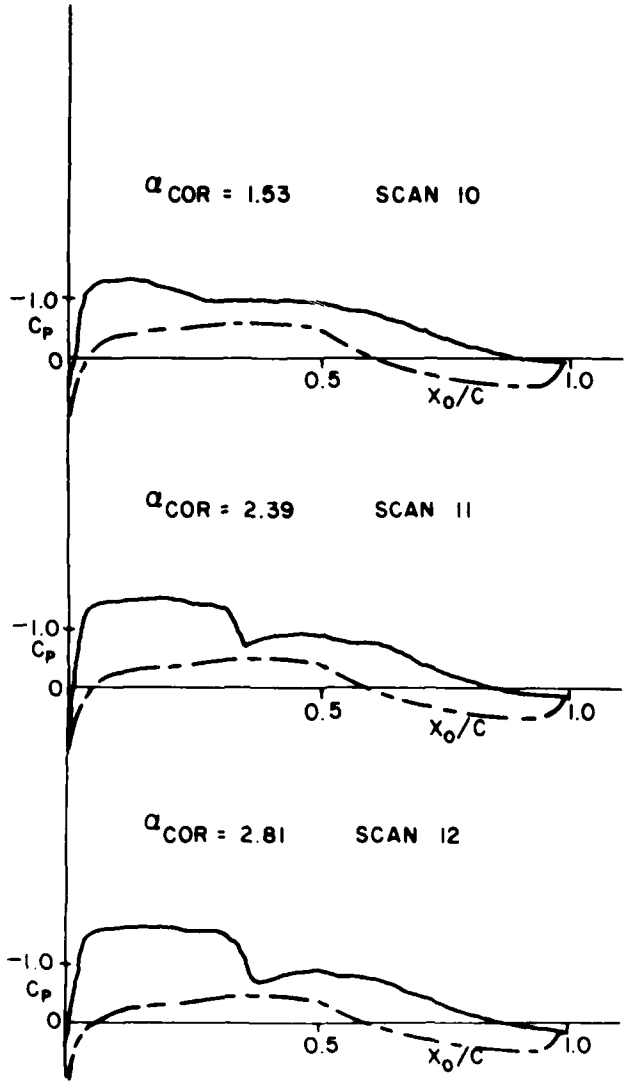

FIG. 7(d) (cont'd): CHORDWISE MEASURED PRESSURE DISTRIBUTION M = 0.66, R_C = 4.17 X 10^6

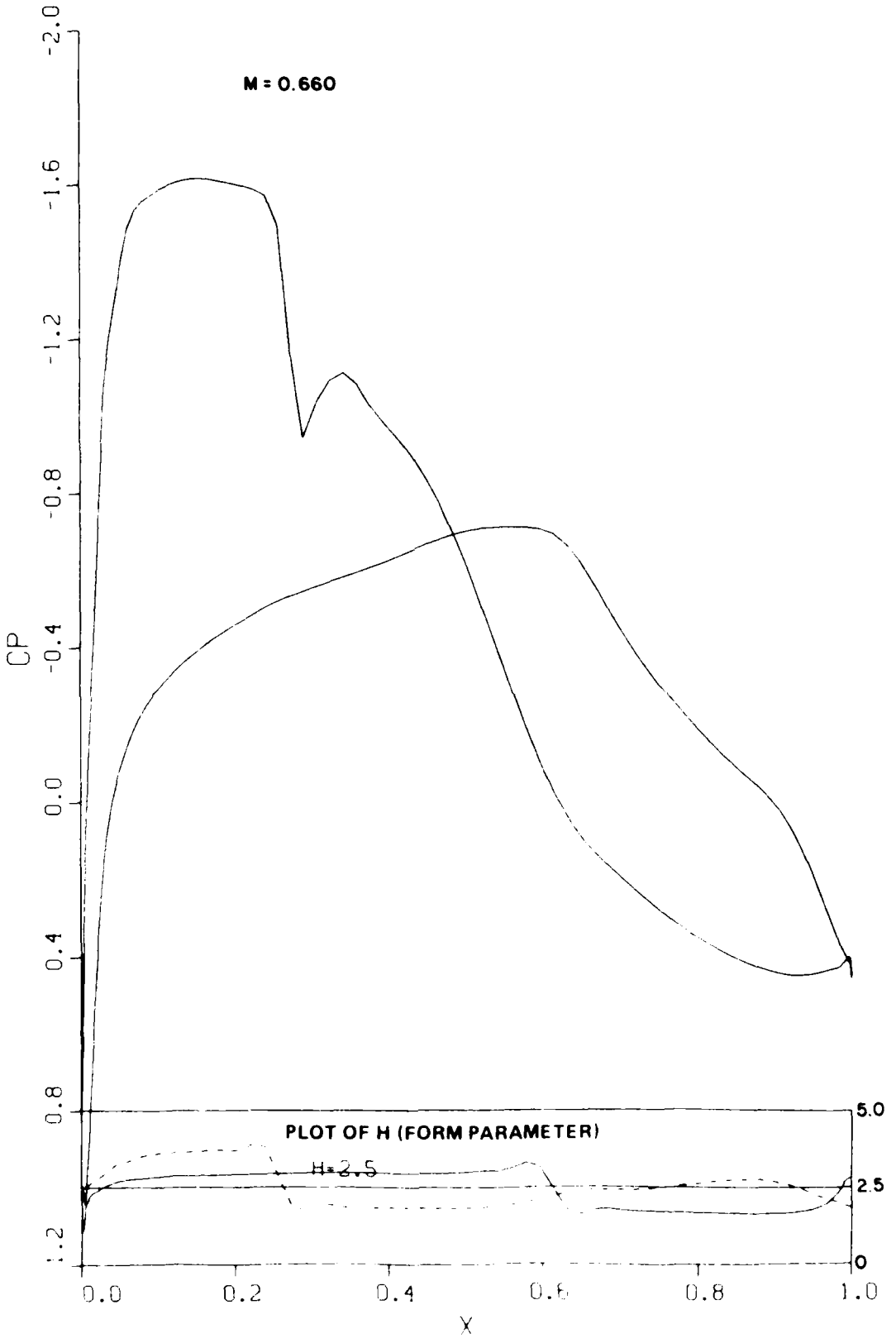

FIG. 7(e): THEORETICAL PRESSURE DISTRIBUTION OBTAINED USING BGK COMPUTER CODE AT C_L = -0.157 AND R_C = 4.17 X 10^6

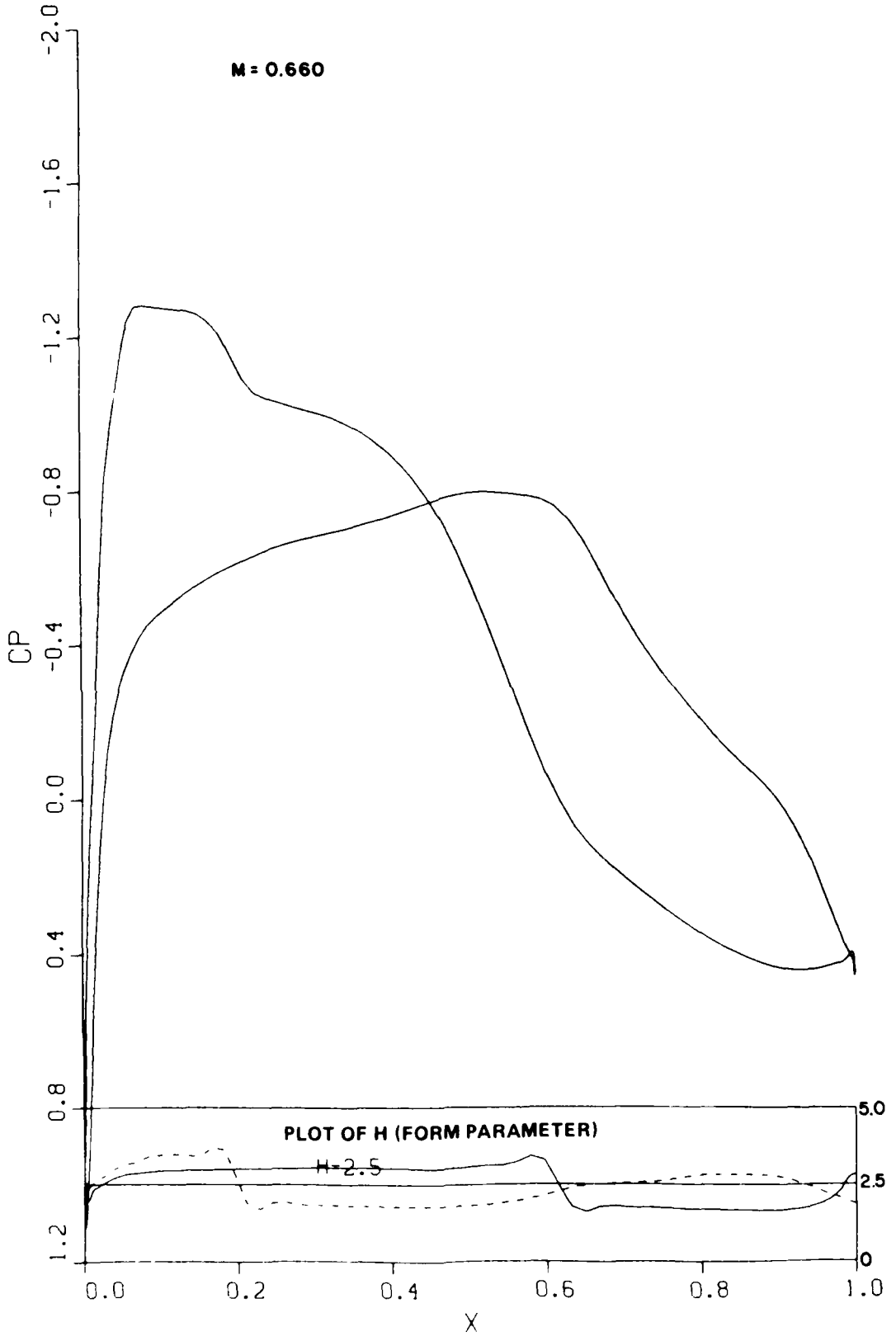

FIG. 7(f): THEORETICAL PRESSURE DISTRIBUTION OBTAINED USING BGK COMPUTER CODE AT C_L = 0.046 AND R_C = 4.17 X 10^6

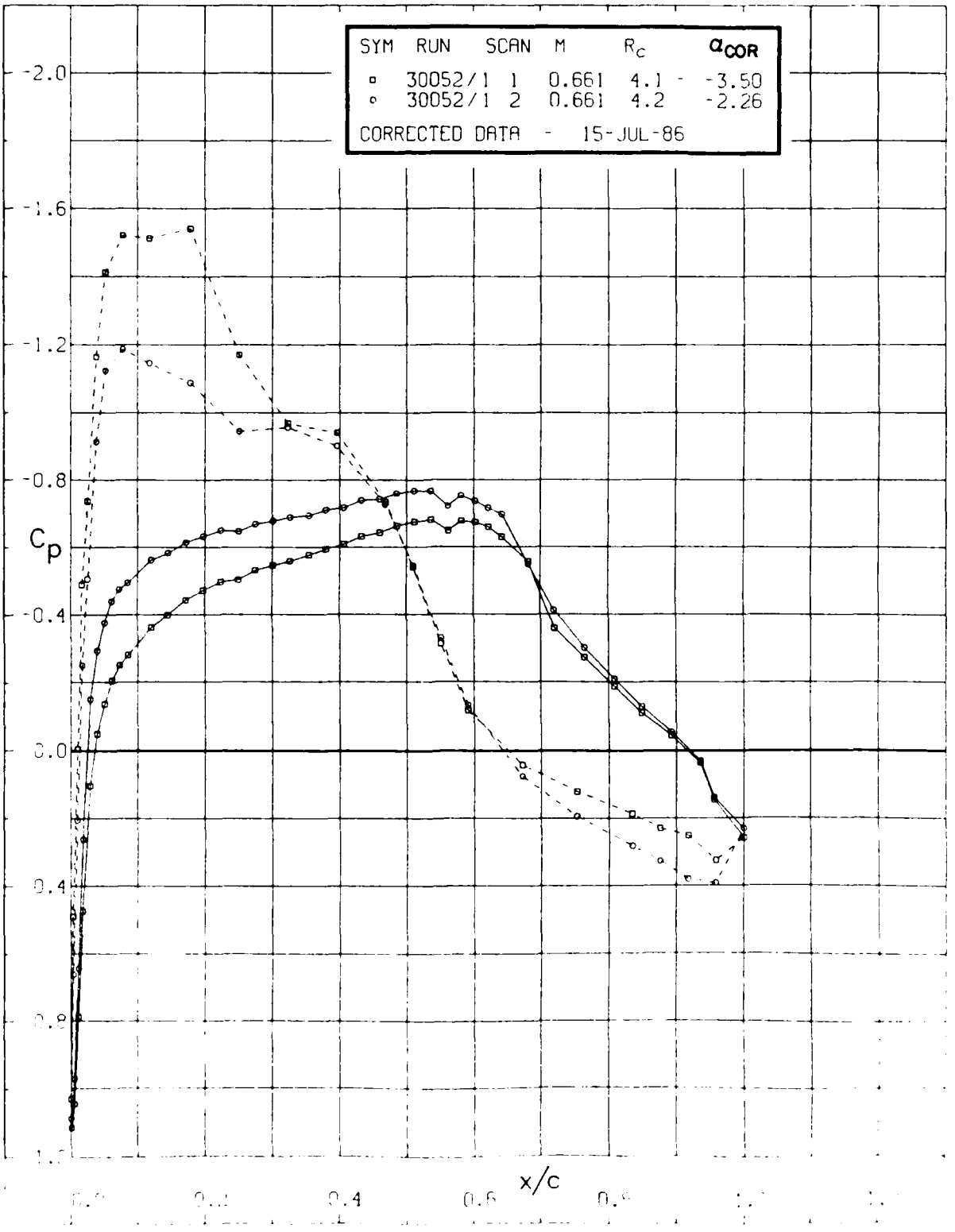

FIG. 7(g): EXPERIMENTAL PRESSURE DISTRIBUTION AT C_L = -0.16, 0.046 AND $R_C = 4.17 \times 10^6$

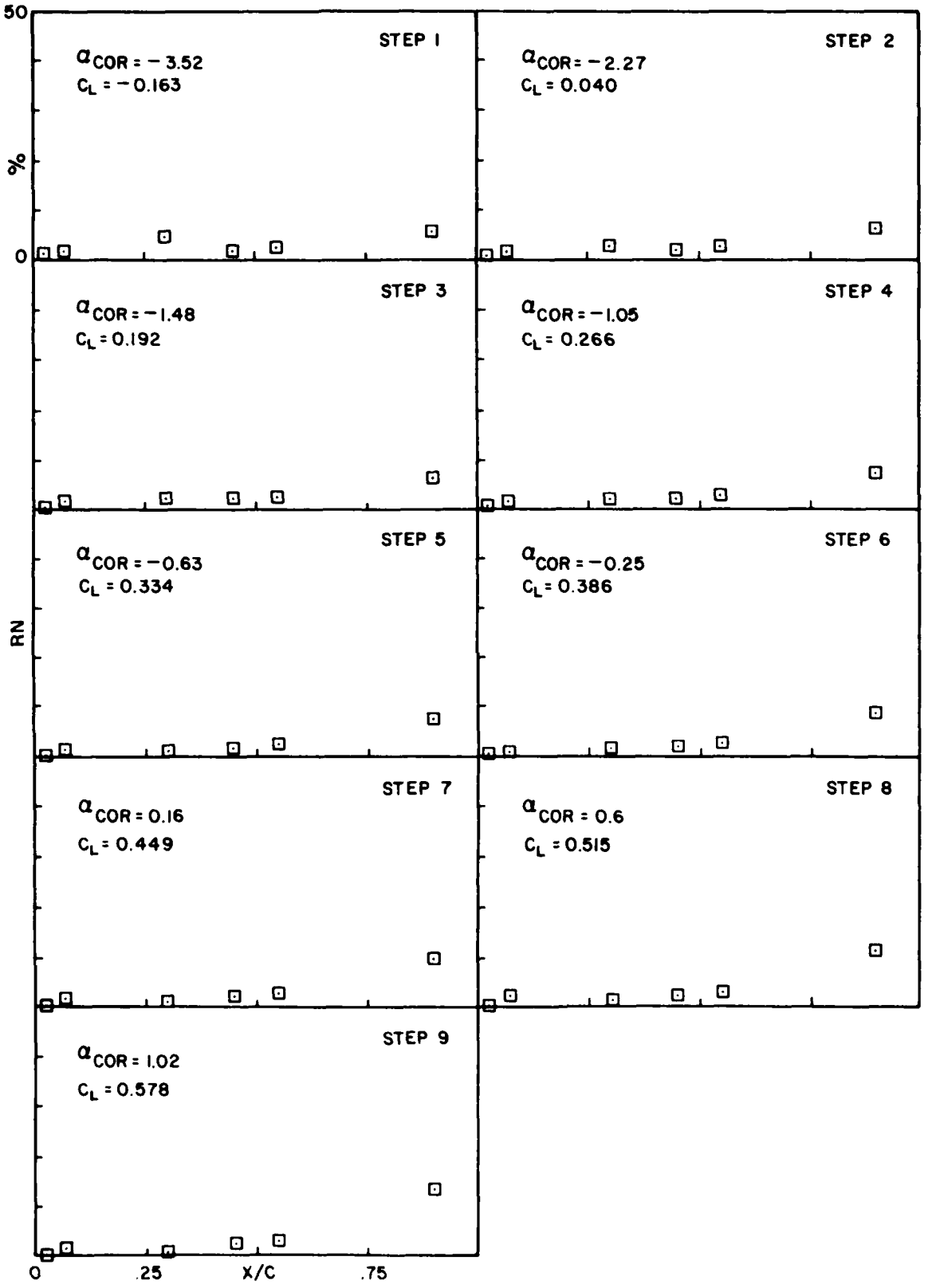

FIG. 8(a): HOT-FILM RECORDS $-3.52 \leq \alpha_{COR} \leq 4.2$, M = 0.66 AND $R_C = 6.67 \times 10^6$

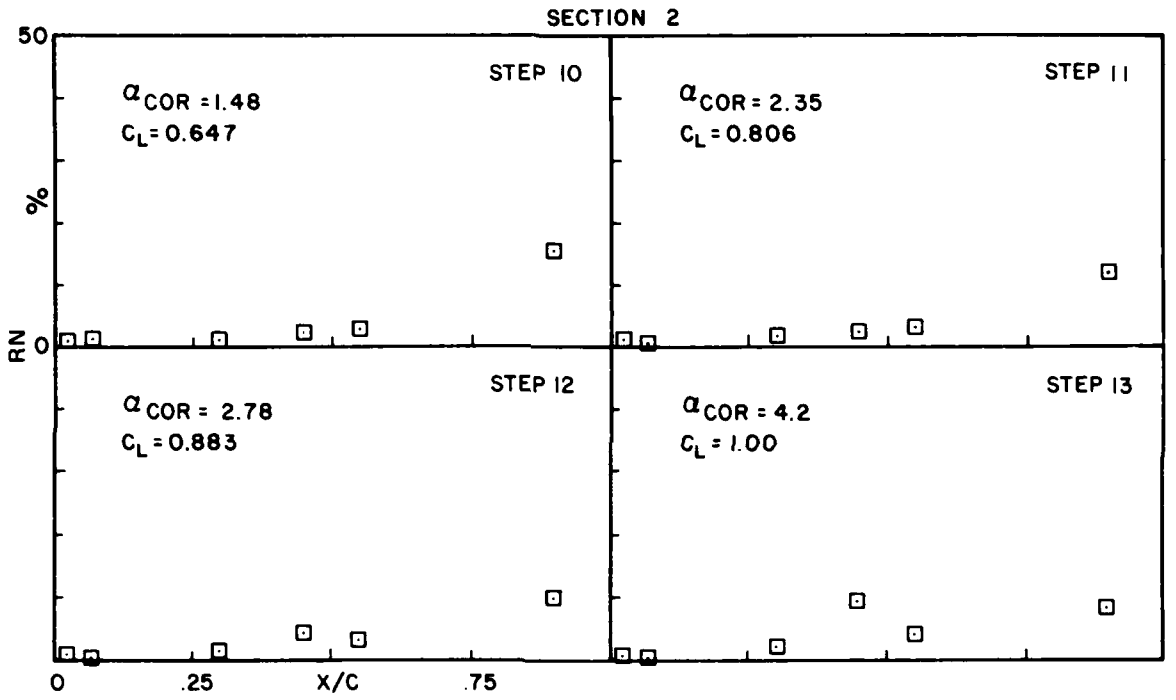

FIG. 8(a) (cont'd): HOT-FILM RECORDS $-3.52 \leqslant \alpha_{COR} \leqslant 4.2$, M = 0.66 AND $R_C = 6.67 \times 10^6$

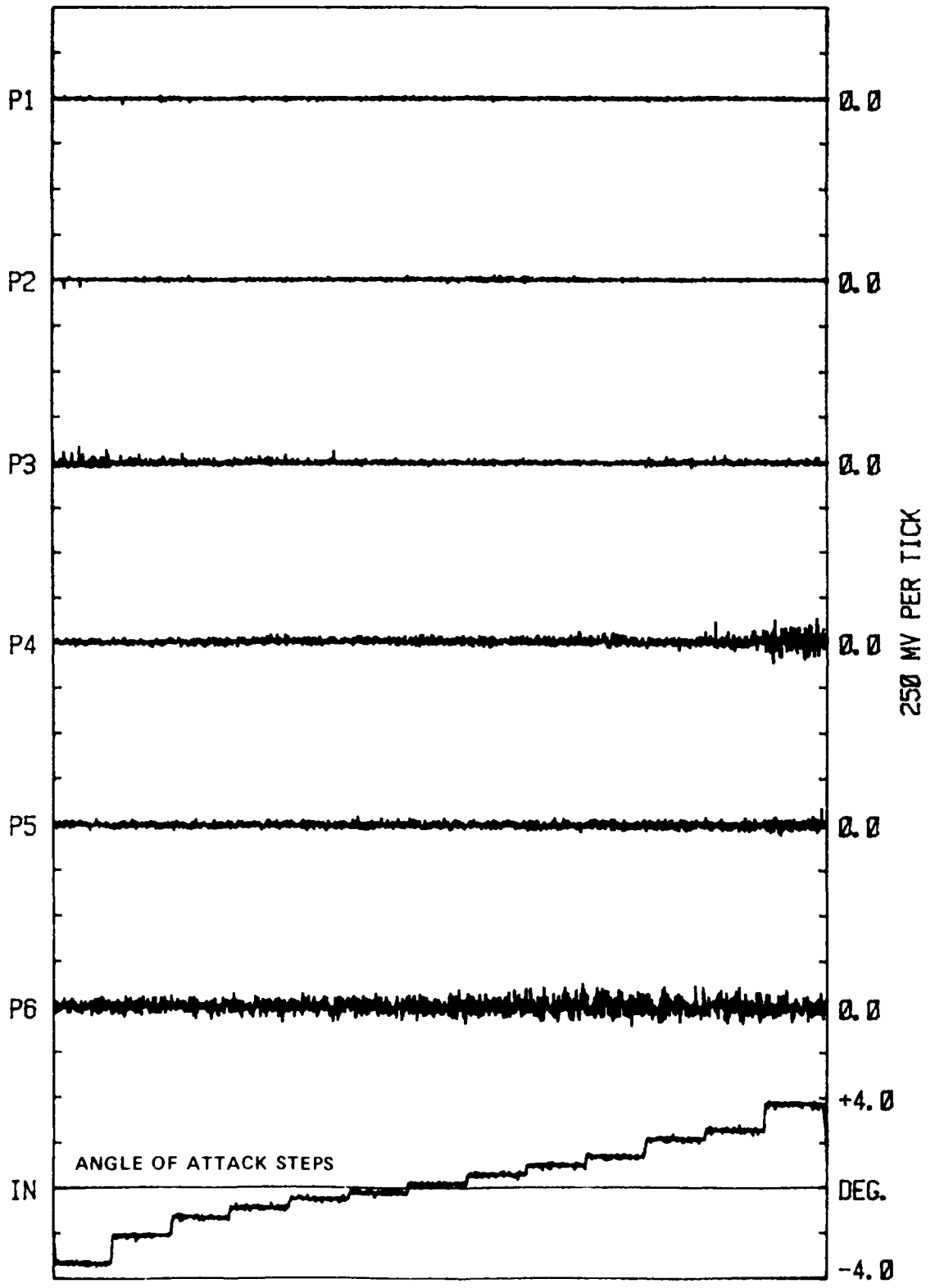

FIG. 8(b): THE AC SIGNAL FROM THE DISA HOT-FILM PROBES

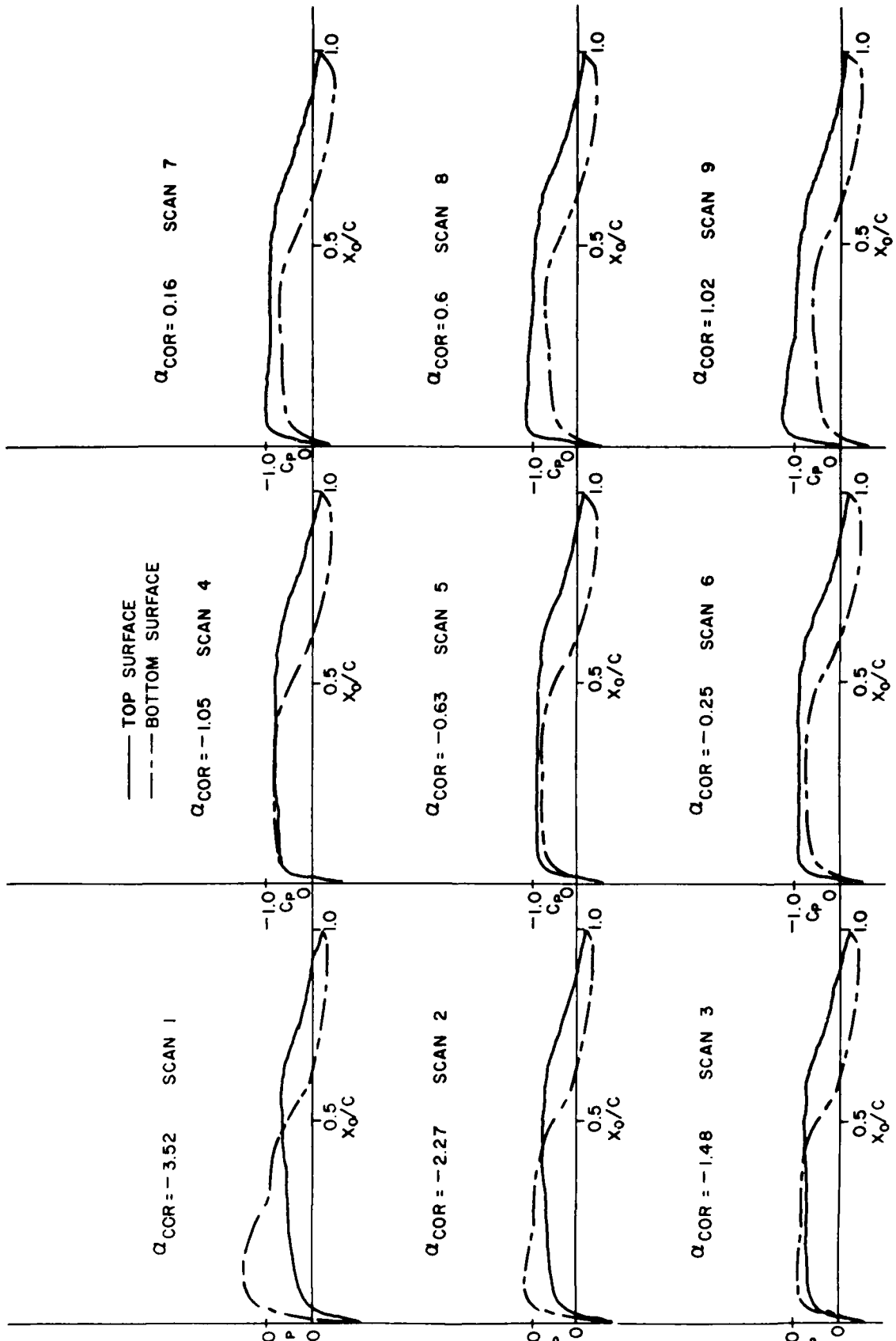

FIG. 8(c): CHORDWISE MEASURED PRESSURE DISTRIBUTION $-3.52 \leqslant \alpha_{COR} \leqslant 4.2$, M = 0.66 and $R_C = 6.67 \times 10^6$

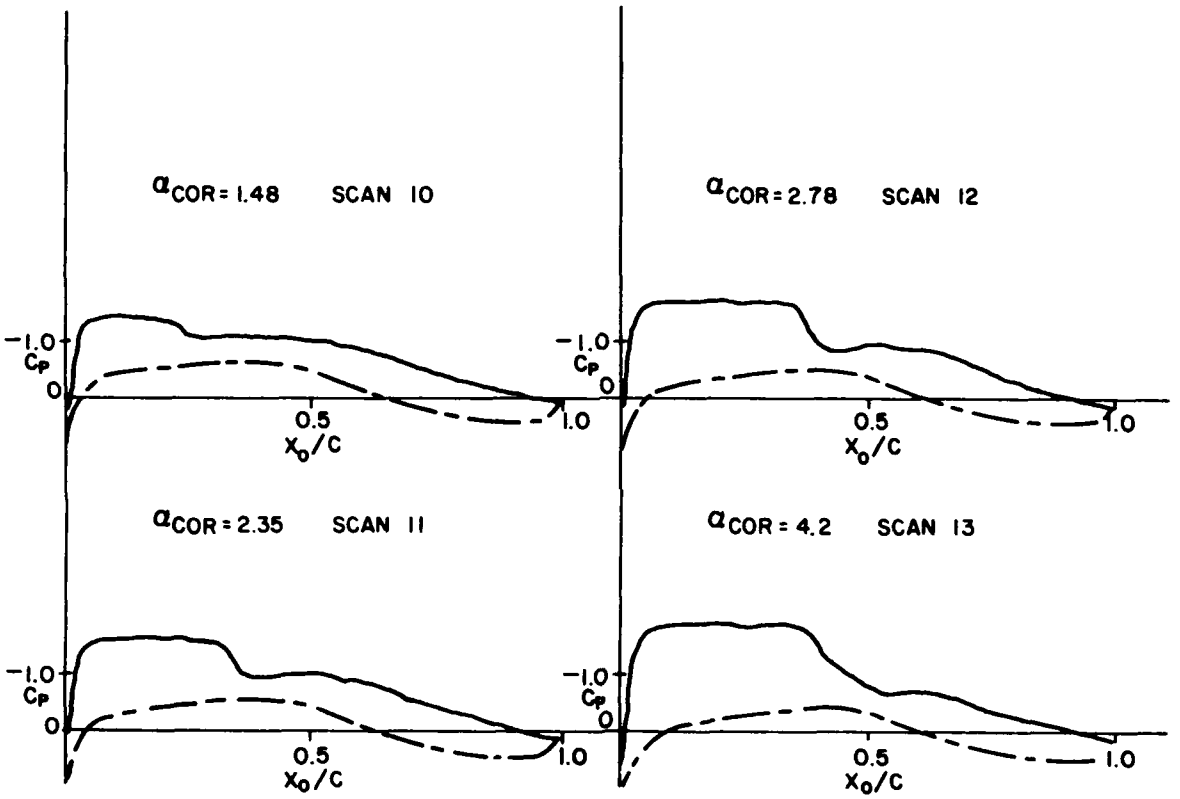

FIG. 8(c) (cont'd): CHORDWISE MEASURED PRESSURE DISTRIBUTION $-3.52 \leq \alpha_{COR} \leq 4.2$, M = 0.66 and $R_C = 6.67 \times 10^6$

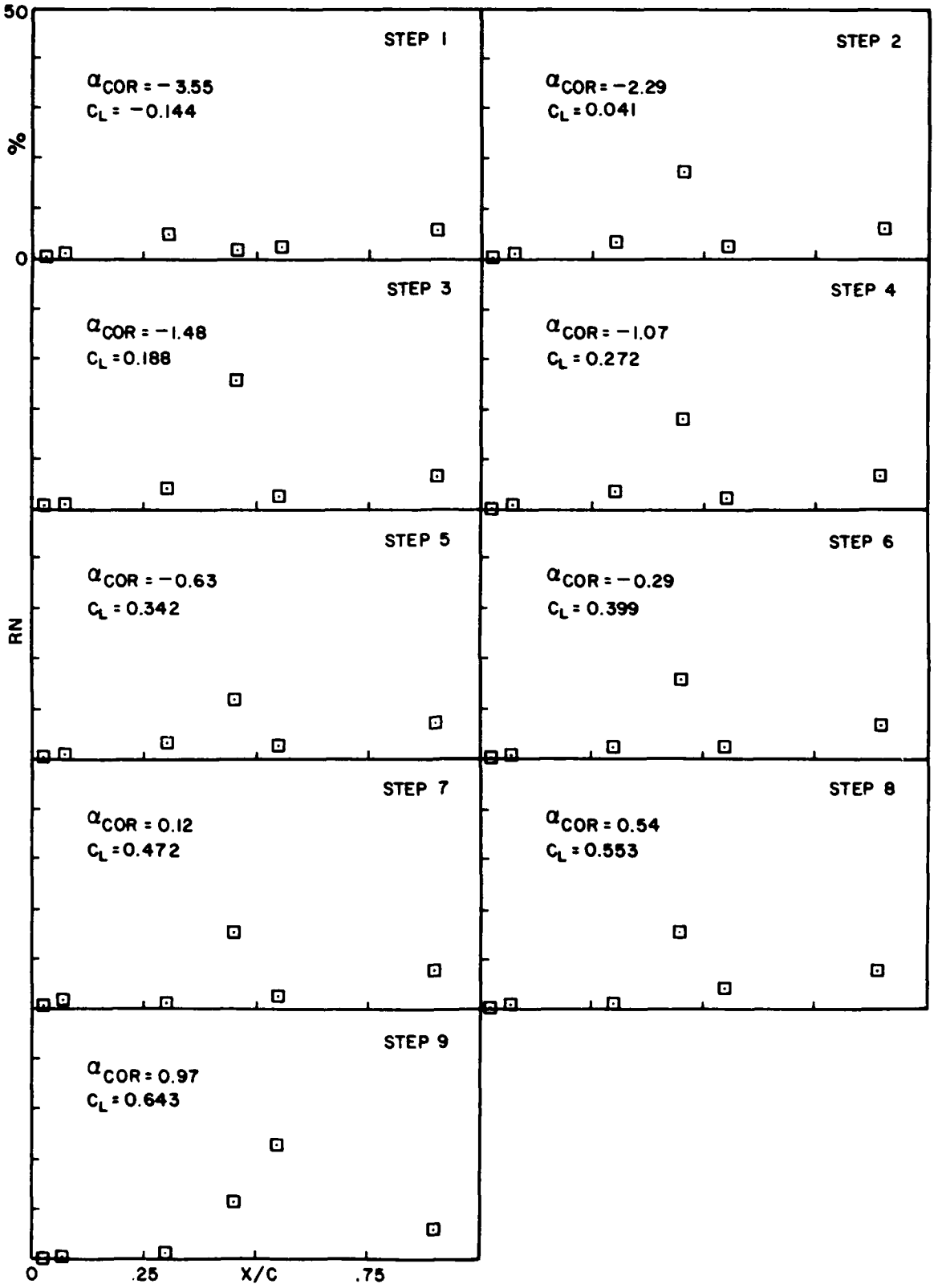

FIG. 9(a): HOT-FILM RECORDS $-3.55 \leqslant \alpha_{COR} \leqslant 4.27$, M = 0.7 AND $R_C = 6.66 \times 10^6$

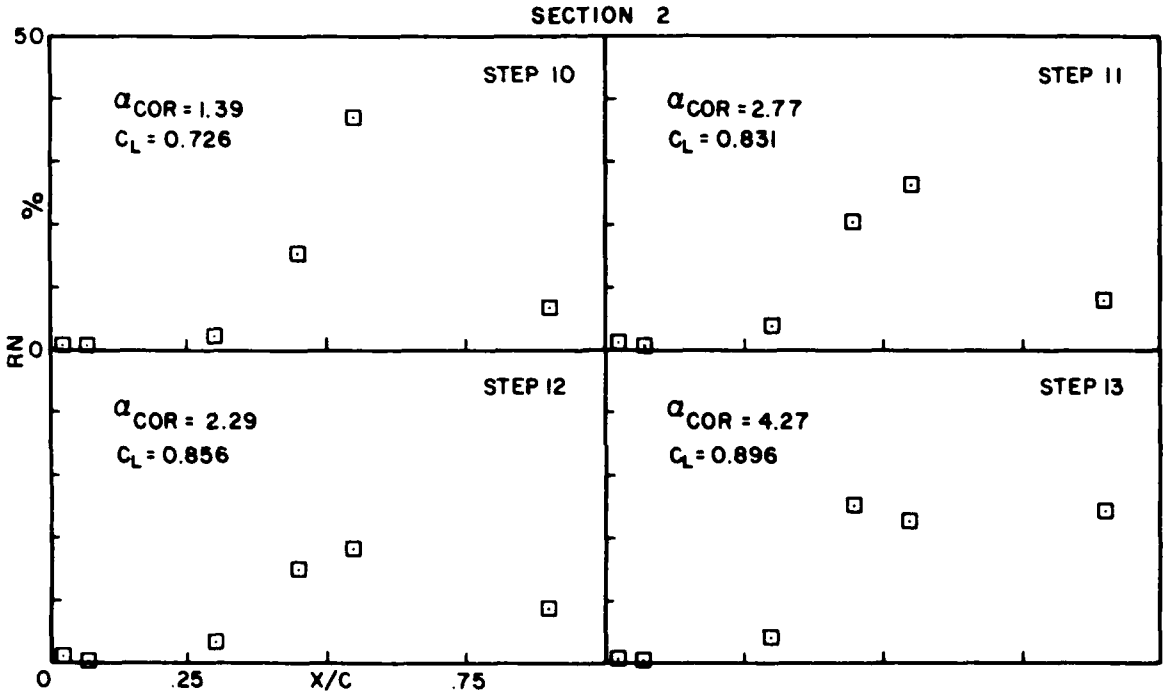

FIG. 9(a) (cont'd): HOT-FILM RECORDS $-3.55 \leqslant \alpha_{COR} \leqslant 4.27$, M = 0.7 AND $R_C = 6.66 \times 10^6$

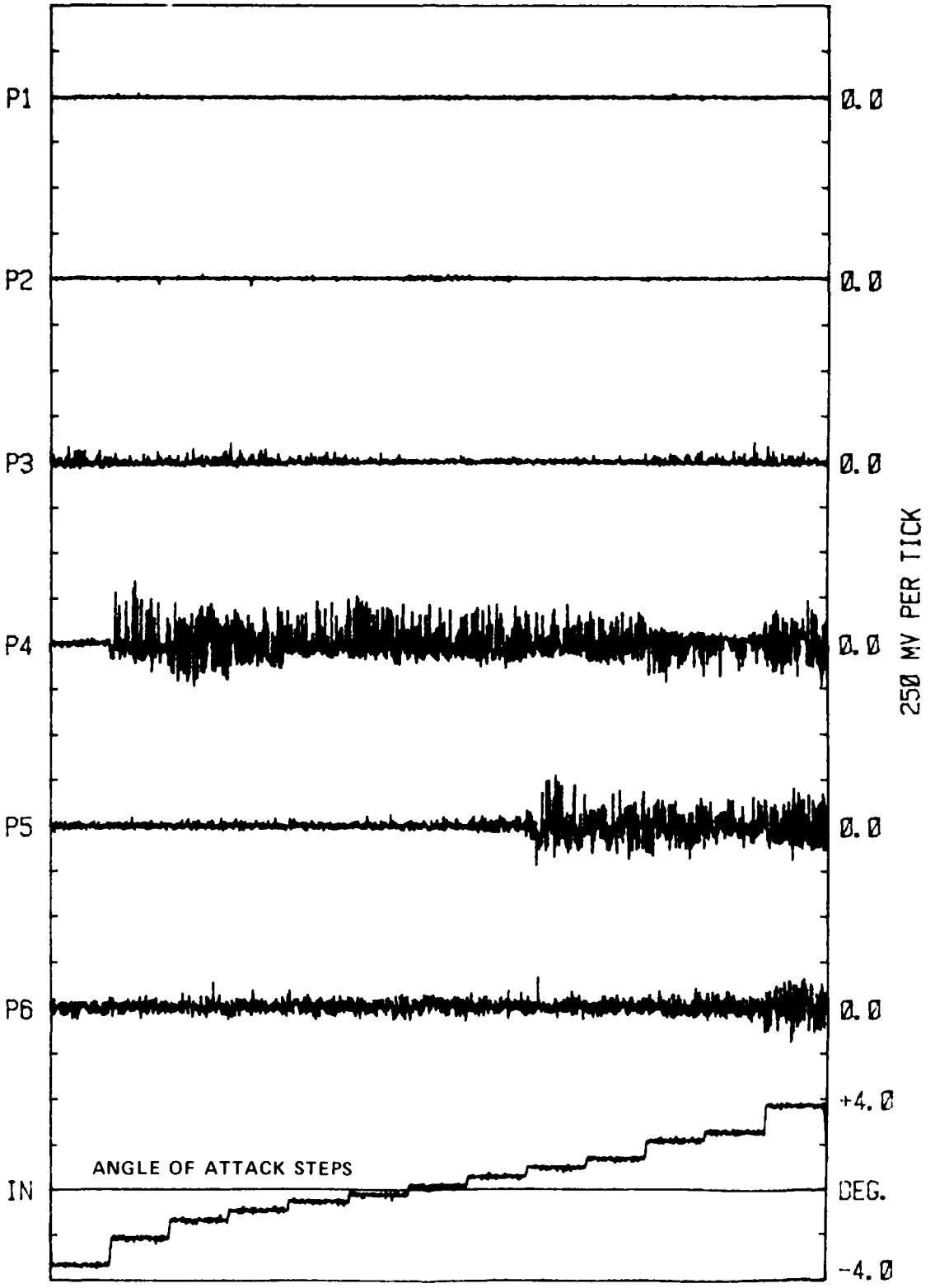

FIG. 9(b): THE AC SIGNAL FROM THE DISA HOT-FILM PROBES

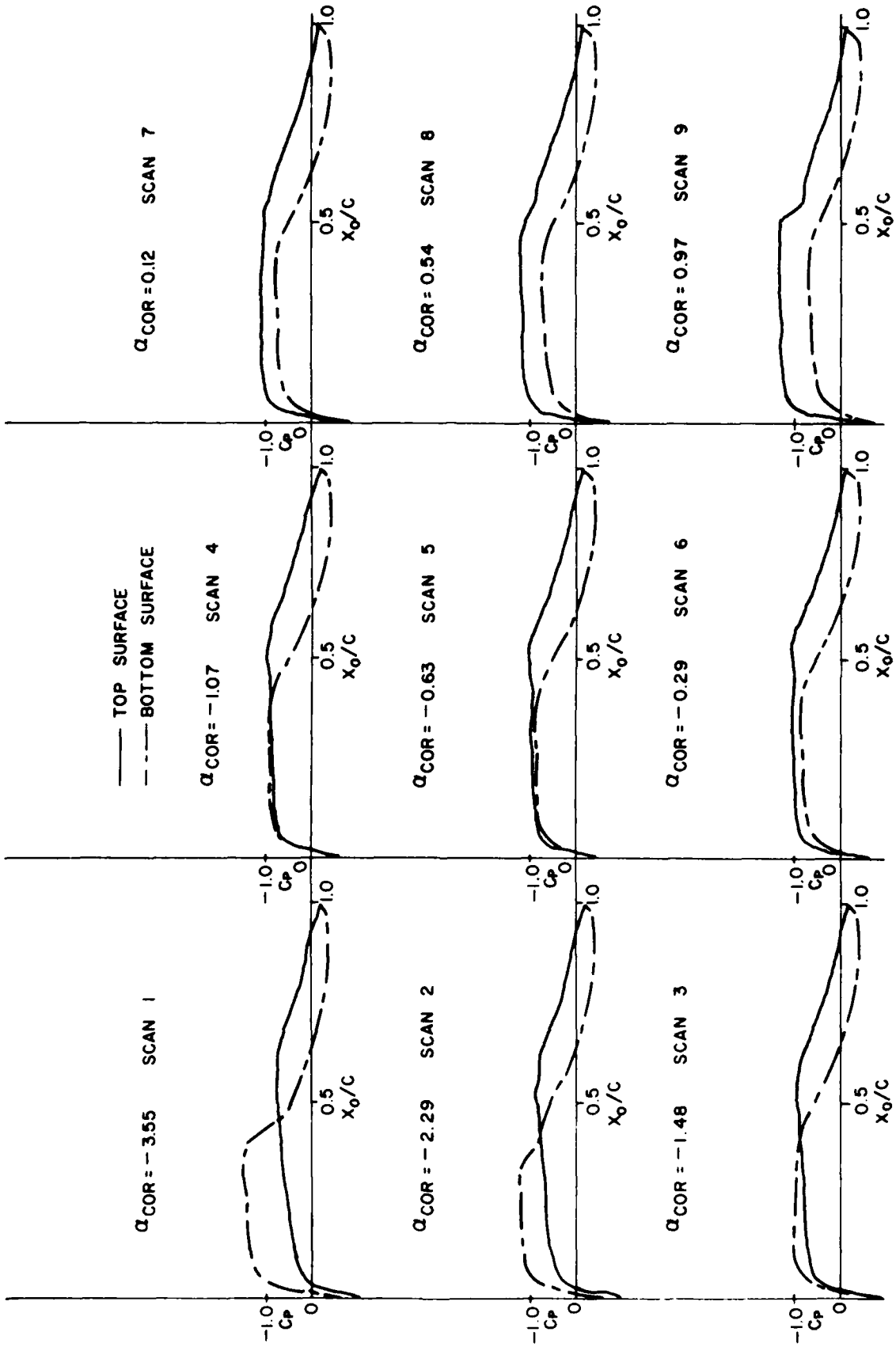

FIG. 9(c): CHORDWISE MEASURED PRESSURE DISTRIBUTION $-3.55 \leqslant \alpha_{COR} \leqslant 4.27$, M = 0.7 AND $R_C = 6.66 \times 10^6$

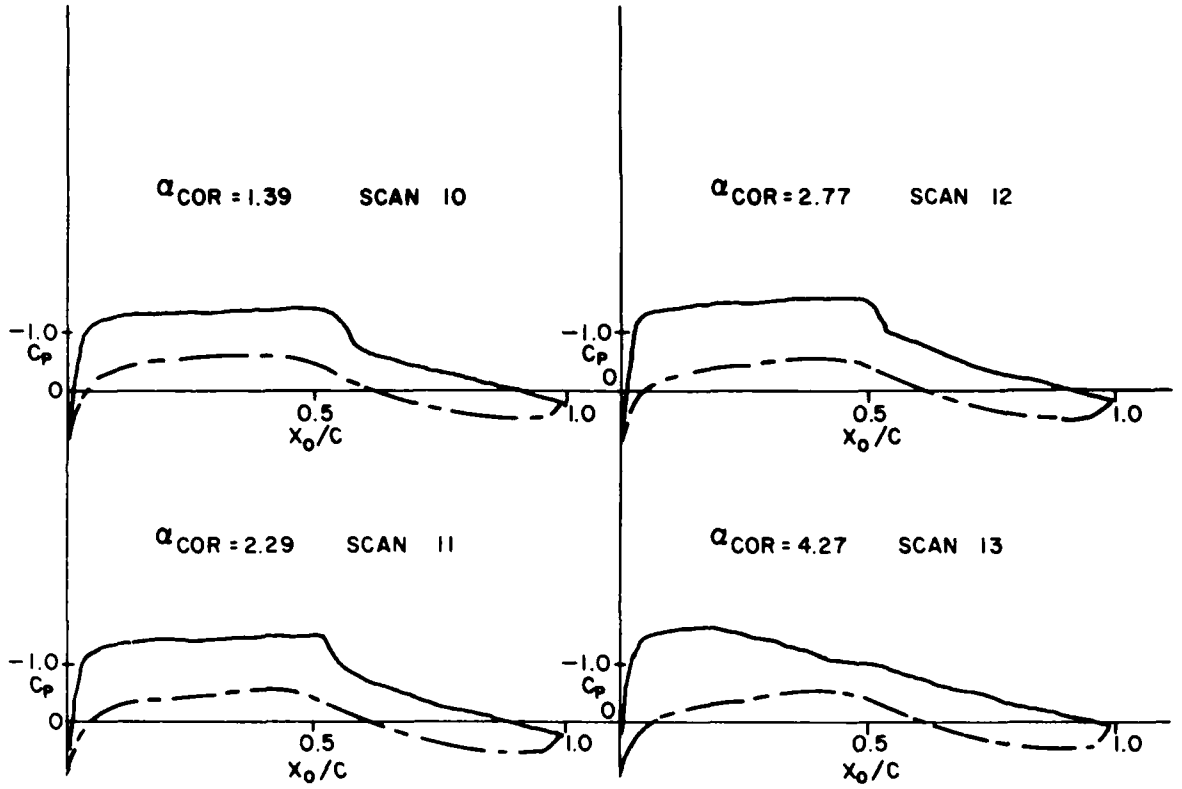

FIG. 9(c) (cont'd): CHORDWISE MEASURED PRESSURE DISTRIBUTION $-3.55 \leqslant \alpha_{COR} \leqslant 4.27$, $M = 0.7$ AND $R_C = 6.66 \times 10^6$

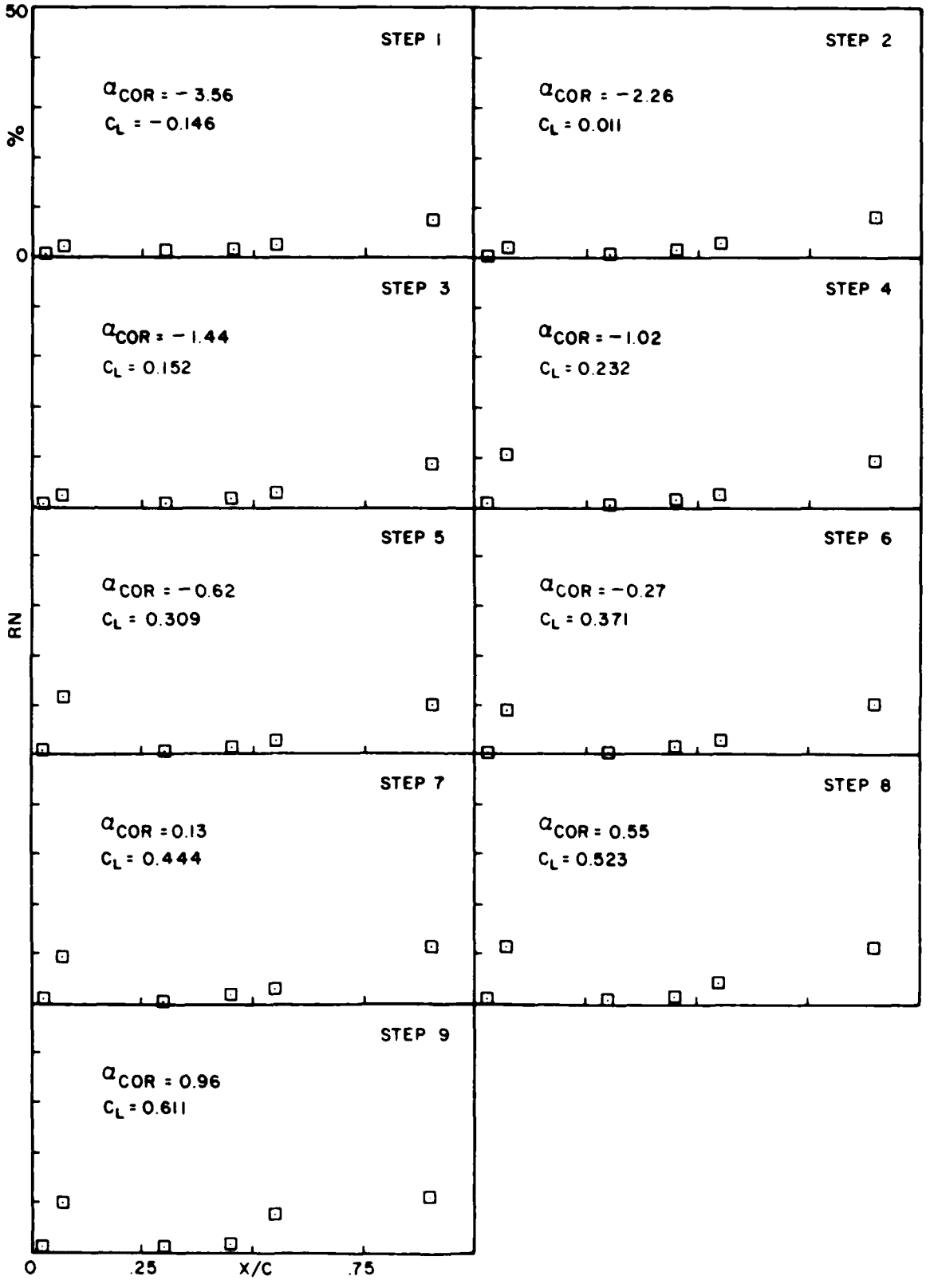

FIG. 10(a): HOT-FILM RECORDS $-3.56 < \alpha_{COR} < 4.28$, M = 0.7 AND $R_C = 9.17 \times 10^6$

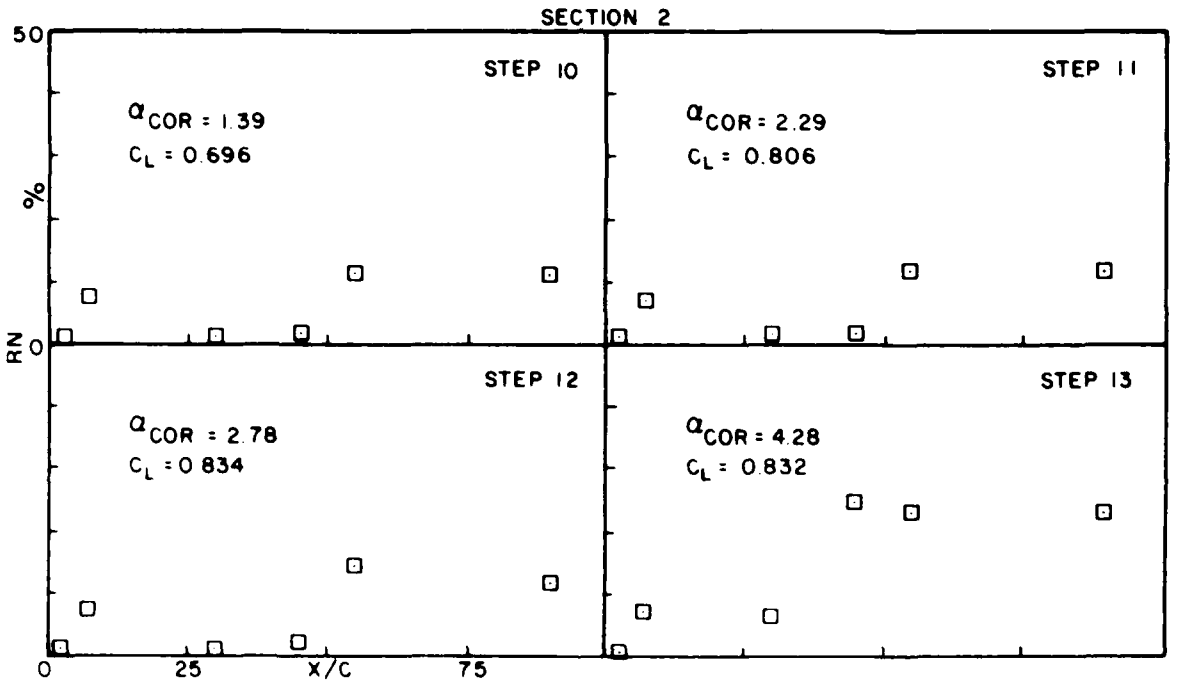

FIG. 10(a) (cont'd): HOT-FILM RECORDS $-3.56 \leq \alpha_{COR} \leq 4.28$, M = 0.7 AND $R_C = 9.17 \times 10^6$

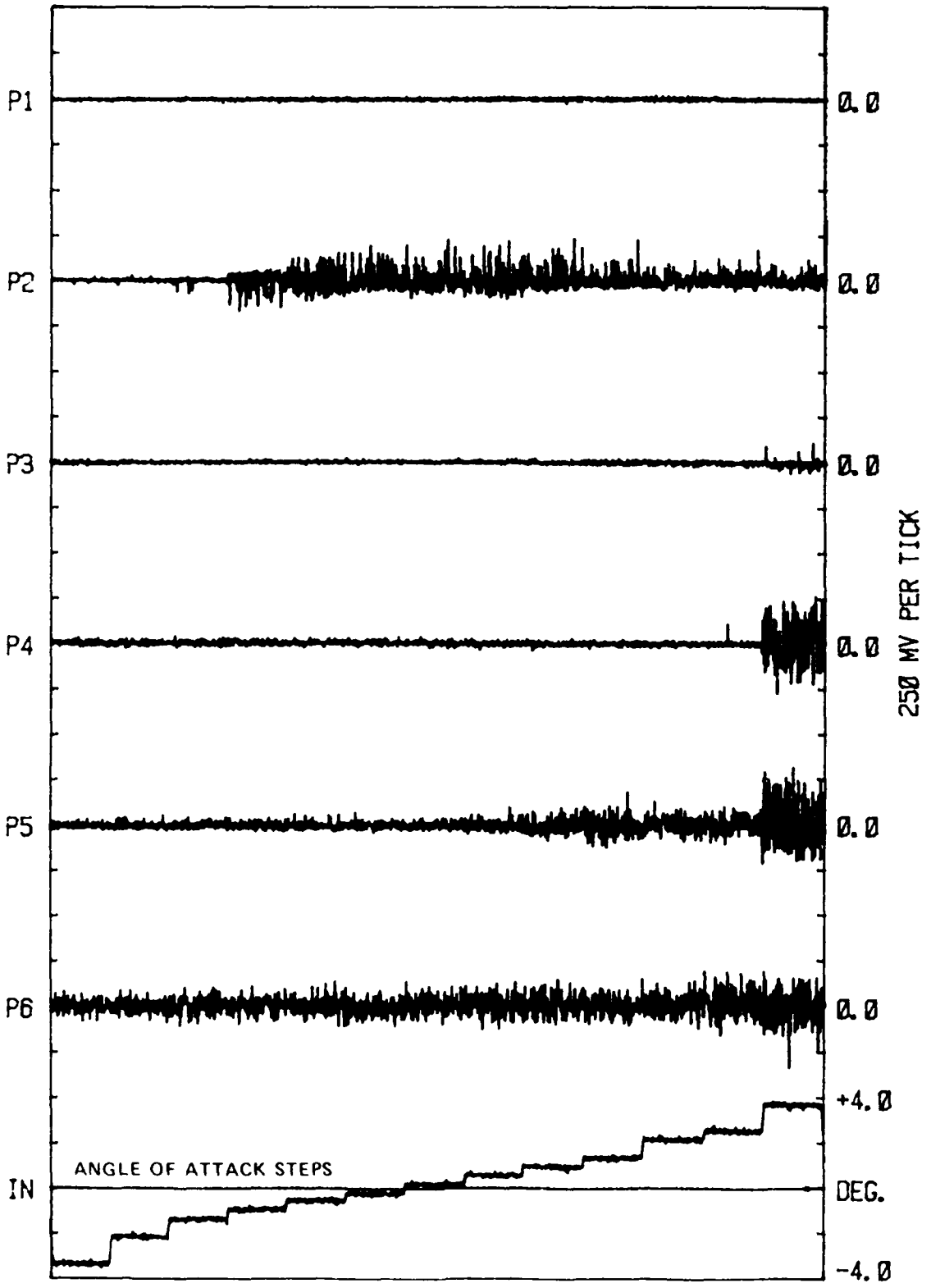

FIG. 10(b): THE AC SIGNAL FROM THE DISA HOT-FILM PROBES

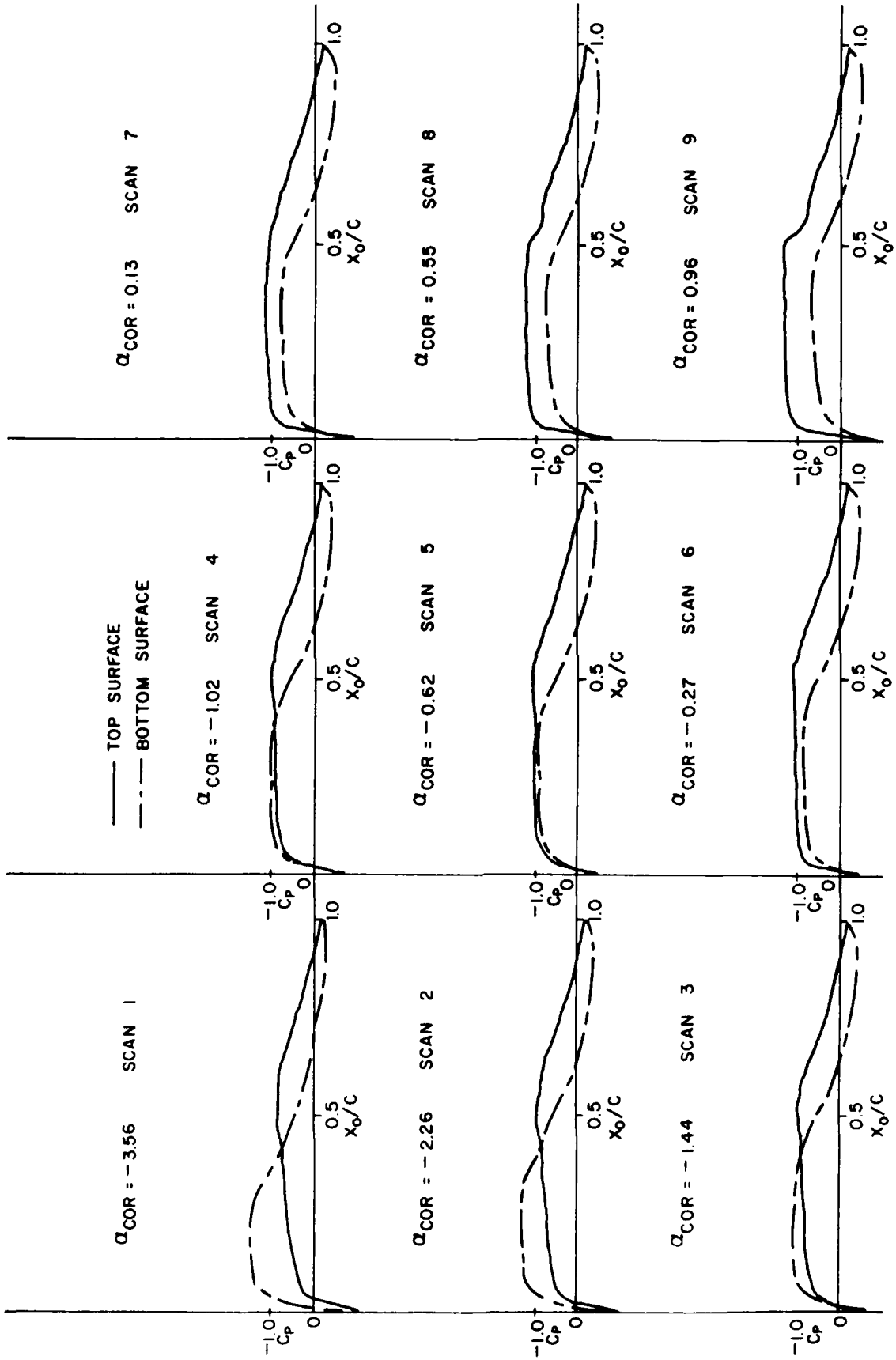

FIG. 10(c): CHORDWISE MEASURED PRESSURE DISTRIBUTION $-3.56 \leqslant \alpha_{COR} \leqslant 4.28$, M = 0.7 AND $R_C = 9.17 \times 10^6$

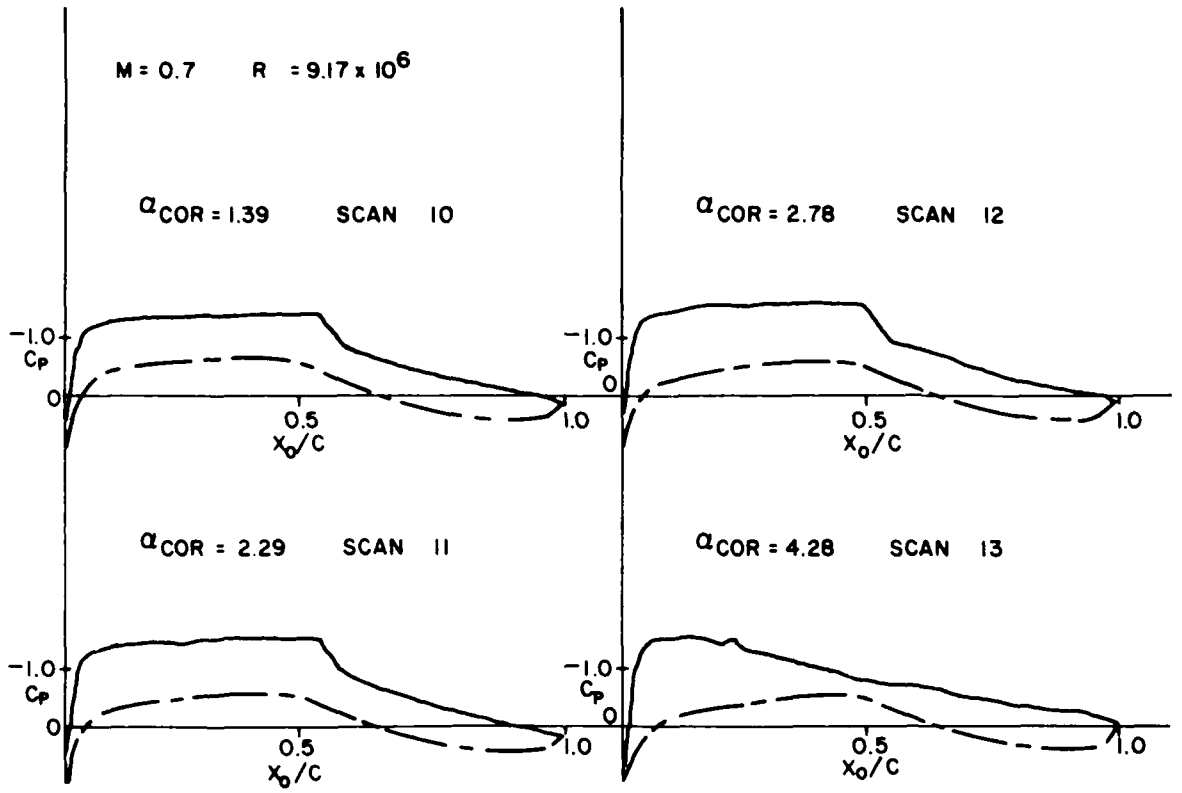

FIG. 10(c) (cont'd): CHORDWISE MEASURED PRESSURE DISTRIBUTION $-3.56 \leqslant \alpha_{COR} \leqslant 4.28$, M = 0.7 AND $R_C = 9.17 \times 10^6$

REPORT DOCUMENTATION PAGE / PAGE DE DOCUMENTATION DE RAPPORT

REPORT/RAPPORT	REPORT/RAPPORT
NAE-AN-45	NRC No. 27892
1a	1b
REPORT SECURITY CLASSIFICATION CLASSIFICATION DE SÉCURITÉ DE RAPPORT	DISTRIBUTION (LIMITATIONS)
UNCLASSIFIED	UNLIMITED
2	3

TITLE/SUBTITLE/TITRE/SOUS-TITRE

The Use of Hot-Film Technique for Boundary Layer Studies on a 21% Thick Airfoil

4

AUTHOR(S)/AUTEUR(S)

M. Khalid

5

SERIES/SÉRIE

Aeronautical Note

6

CORPORATE AUTHOR/PERFORMING AGENCY/AUTEUR D'ENTREPRISE/AGENCE D'EXÉCUTION

7

SPONSORING AGENCY/AGENCE DE SUBVENTION

National Research Council of Canada
National Aeronautical Establishment / High Speed Aerodynamics Laboratory

8

DATE	FILE/DOSSIER	LAB. ORDER COMMANDE DU LAB.	PAGES	FIGS/DIAGRAMMES
May 1987			46	10
9	10	11	12a	12b

NOTES

13

DESCRIPTORS (KEY WORDS)/MOTS-CLÉS

1. Hot-Film Studies 2. Transition Studies 3. Boundary Layers

14

SUMMARY/SOMMAIRE

A heat transfer method of studying boundary layer flows over airfoils at transsonic test conditions has been investigated. The method employs very thin DISA hot-film gauges housing Constant Temperature Anemometer probes. Provided that the thickness dimension of the films remains less than the critical disturbances height for inducing transition of the laminar boundary layer, the heat transfer response from the films, positioned carefully on the model surface, can be studied to determine the boundary layer characteristics. Results from an application study on a 21% thick laminar flow airfoil model are presented and discussed.

15

END

10-87

DTIC